



## *Early Pliocene paleovalley incision during early Rio Grande evolution in southern New Mexico*

D. J. Koning, A. P. Jochems, and M.T. Heizler

2018, pp. 93-108. <https://doi.org/10.56577/FFC-69.93>

Supplemental data: <https://nmgs.nmt.edu/repository/index.cfml?rid=2018001>

*in:*

*Las Cruces Country III*, Mack, Greg H.; Hampton, Brian A.; Ramos, Frank C.; Witcher, James C.; Ulmer-Scholle, Dana S., New Mexico Geological Society 69<sup>th</sup> Annual Fall Field Conference Guidebook, 218 p.

<https://doi.org/10.56577/FFC-69>

---

*This is one of many related papers that were included in the 2018 NMGS Fall Field Conference Guidebook.*

---

### **Annual NMGS Fall Field Conference Guidebooks**

Every fall since 1950, the New Mexico Geological Society (NMGS) has held an annual [Fall Field Conference](#) that explores some region of New Mexico (or surrounding states). Always well attended, these conferences provide a guidebook to participants. Besides detailed road logs, the guidebooks contain many well written, edited, and peer-reviewed geoscience papers. These books have set the national standard for geologic guidebooks and are an essential geologic reference for anyone working in or around New Mexico.

### **Free Downloads**

NMGS has decided to make peer-reviewed papers from our Fall Field Conference guidebooks available for free download. This is in keeping with our mission of promoting interest, research, and cooperation regarding geology in New Mexico. However, guidebook sales represent a significant proportion of our operating budget. Therefore, only *research papers* are available for download. *Road logs*, *mini-papers*, and other selected content are available only in print for recent guidebooks.

### **Copyright Information**

Publications of the New Mexico Geological Society, printed and electronic, are protected by the copyright laws of the United States. No material from the NMGS website, or printed and electronic publications, may be reprinted or redistributed without NMGS permission. Contact us for permission to reprint portions of any of our publications.

One printed copy of any materials from the NMGS website or our print and electronic publications may be made for individual use without our permission. Teachers and students may make unlimited copies for educational use. Any other use of these materials requires explicit permission.

*This page is intentionally left blank to maintain order of facing pages.*

# EARLY PLIOCENE PALEOVALLEY INCISION DURING EARLY RIO GRANDE EVOLUTION IN SOUTHERN NEW MEXICO

DANIEL J. KONING, ANDY P. JOCHEMS, AND MATTHEW T. HEIZLER

New Mexico Bureau of Geology and Mineral Resources, 801 Leroy Place, Socorro, NM, 87801, dan.koning@nmt.edu

**ABSTRACT**—Stratigraphic relations in the Truth or Consequences area indicate that the early Rio Grande incised and backfilled twice over 0.6 my, forming two 20-m-deep paleovalleys, shortly after this paleoriver propagated into southern New Mexico. Paleovalley incision is recognized by buttress unconformities between different-aged, lithologically distinctive axial and piedmont deposits. Older (pre-paleovalley) deposits correlate to the Palomas Formation basal transitional unit (map unit Tplt), which includes western-derived piedmont deposits and some of the earliest Rio Grande deposits in the Palomas and Engle Basins. The first (older) paleovalley was backfilled with axial-fluvial sediment consisting of a coarse-grained, basal conglomerate overlain by sandstone and pebbly sandstone; all gravel was locally derived from highlands surrounding the Engle Basin. The second paleovalley fill is distinctive because it contains extrabasinal, coarser (cobble-rich) conglomerate. To the west, the top of the Tplt unit is overlain by coarser-grained and lesser cemented piedmont deposits of the Palomas Formation. These volcanoclastic deposits interfinger eastward with axial-fluvial deposits overlying both aforementioned paleovalleys; these younger axial-fluvial deposits are composed of sand with 5–20% pebbly beds that lack extrabasinal gravel. Radiometric dating of basalt clasts and cryptomelane provide age control for paleovalley formation. A basalt clast dated at  $5.06 \pm 0.02$  Ma ( $^{40}\text{Ar}/^{39}\text{Ar}$  age), collected ~4 m below the top of Tplt, provides a maximum age for both the top of this unit and incision of the older paleovalley. Cryptomelane precipitated at the top of the older paleovalley fill is  $4.87 \pm 0.05$  (previously published  $^{40}\text{Ar}/^{39}\text{Ar}$  age). Thus, incision and back-filling of the first paleovalley happened between 5.1 and 4.87 Ma, and incision of the second, nested paleovalley occurred after 4.87 Ma. A basalt cobble collected 6 m above the base of the coarse-grained, lesser-cemented piedmont deposits returned an  $^{40}\text{Ar}/^{39}\text{Ar}$  age of  $4.49 \pm 0.03$  Ma. This stratigraphic horizon projects to 10–12 m above the base of the younger axial-fluvial unit that overlies the second paleovalley; the horizon also underlies (by at least 15 m) the ~3.6–3.3 Ma Repenning fossil site. Thus, aggradation of the second paleovalley continued to ca. 4.5 Ma. The relatively quick succession of two ~20-m-deep incision/backfilling events within 0.6 my, each incising to a similar base level, suggests a paleoclimatic driver that caused notable fluctuations in sediment-water discharge ratios similar to later Pleistocene events. We propose that a similar buried paleovalley may exist between the Palomas and Mesilla Basins, which might explain the general lack of pre-3.6 Ma axial-fluvial deposits in that region.

## INTRODUCTION

In the early Pliocene, the Rio Grande propagated southward between Socorro and the Las Cruces area, integrating several previously closed (endorheic) basins. Concomitantly, the Colorado River extended downstream between the Grand Canyon and the Gulf of California (House et al., 2008; Pearthree and House, 2014). What drove this downstream-directed integration of the Rio Grande is controversial, and explanations have been proposed involving tectonic changes (Connell et al., 2005), paleoclimatic factors (Koning et al., 2016a, b), epeirogenic uplift (Kottlowski, 1953; Repasch et al., 2017), or combinations of these (Repasch et al., 2017).

The existence of paleovalleys in Truth or Consequences (TorC), and what caused them, are germane to the early Pliocene integration of the Rio Grande. This paper documents the incision and subsequent backfilling of two distinct, 20-m-deep paleovalleys that formed shortly after the ancestral Rio Grande entered the northern Palomas Basin in southern New Mexico. We present new stratigraphic and sedimentologic data documenting the existence of an older paleovalley and a younger, inset paleovalley. New  $^{40}\text{Ar}/^{39}\text{Ar}$  ages determinations and published age control (Koning et al., 2016a) constrain the cutting and backfilling of the first paleovalley to 5.1–4.87 Ma and the younger paleovalley to between 4.87 and ca. 4.5 Ma. We discuss possible mechanisms that may have driven paleovalley

incision and backfilling. Lastly, we propose that a similar paleovalley may have linked the Palomas and Mesilla Basins, which may explain the paucity of early Rio Grande deposits downstream of the Palomas Basin.

## Geographic and geologic setting

We examined exposures on the bluffs and hilly terrain that lie immediately north of downtown TorC and Williamsburg, New Mexico (Fig. 1). Williamsburg is located 3 km WSW of downtown TorC. The study area lies on a structural high between the Palomas and Engle Basins, which is a continuation of the same structural block as the Mud Springs Mountains immediately to the northwest. A major northwest-trending, basin-bounding normal fault, called the Mud Springs fault, separates the strata exposed in these bluffs from younger strata to the southwest. The Mud Springs fault merges southward with the Hot Springs fault and continues southward to near the town of Arrey as the Caballo fault, which lies at the western foot of the Caballo Mountains (Fig. 1). The Palomas Basin and adjoining basins to the north and south, the Engle and Hatch-Rincon Basins, respectively, are underlain by rift-basin fill of the Santa Fe Group (Fig. 1). Most of the Santa Fe Group exposed in the Engle and Palomas Basins is Plio-Pleistocene in age (Seager et al., 1984; Lozinsky and Hawley, 1986a, b; Morgan and Lucas, 2012; Morgan et al., 2011; Morgan and Harris, 2015;

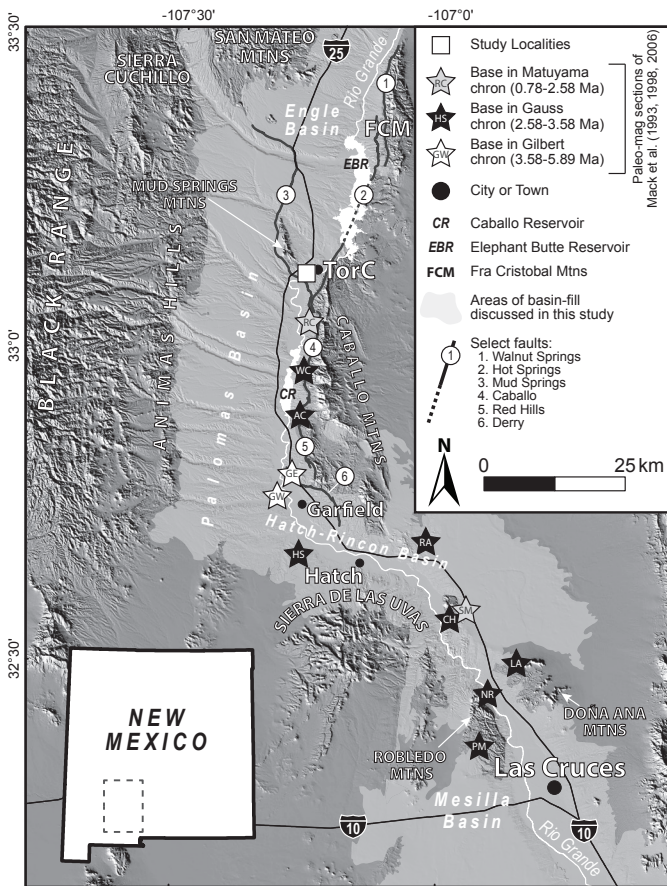


FIGURE 1. Map showing the study area relative to geographic features and Rio Grande rift basins in southern New Mexico. The study localities lie on a structural high between the Palomas and Engle Basins, near the town of Truth or Consequences (TorC). Light gray shade denotes clastic basin fill of the Santa Fe Group. Sites to south where previous magnetostratigraphic analyses were conducted are shown by star symbols, which are color-coded according to interpreted geomagnetic polarity chron at the base of a specific section (Mack et al., 1993, 1998, 2006). Depicted sites measured Plio-Pleistocene sediments that mostly or entirely consisted of axial-fluvial facies. Site abbreviations are: RC=Red Canyon, WC=Wild Horse Canyon, AC=Apache Canyon, GC=Green Canyon (also referred to as Garfield East), GW=Garfield West, HS=Hatch Siphon, RA=Rincon Arroyo, CD=Cedar Hill, LA=Lucero Arroyo, NE=North-east Robledo, and PM=Picacho Mountain.

Mack et al., 1993, 1998, 2006). Miocene strata is exposed in much of the Hatch-Rincon Basin and on the distal (western) hanging-wall ramp of the Palomas Basin (Seager and Hawley, 1973; Seager, 1995; Seager et al., 1982; Jochems, 2015; Koning et al., 2015; Jochems and Koning, 2015, 2016, 2017). Rift basin fill near TorC consists of the following lithofacies assemblages: 1) east-sloping piedmont (with Black Range detrital provenance), 2) local alluvial fans surrounding the Mud Springs Mountains, 3) axial-fluvial deposits of the ancestral Rio Grande, and 4) alluvial-fan sediment derived from the Caballo Mountains (Foster, 2009; Mack et al., 2012; Seager and Mack, 2003; and Seager, 2015; Jochems and Koning, 2015). Plio-Pleistocene strata is called the Palomas Formation in the Palomas and Engle Basins but named the Camp Rice Formation in the Hatch-Rincon and Mesilla Basins (e.g., Seager and Hawley, 1973; Seager et al., 1982; Seager and Mack, 1991; Seager, 1995).

## Rio Grande rift axial-river system

In southern New Mexico, there is no evidence of an axial river (i.e., paleo Rio Grande) in rift basins prior to the Pliocene (e.g., Mack, 2004; Connell et al., 2005). Rather, the existence of upper Miocene playa lake deposits in the Hatch-Rincon area (Hawley et al., 1969; Seager et al., 1971, 1975; Seager and Hawley, 1973; Mack et al., 1994; Mack, 2004) and near TorC (Jochems and Koning, 2015) indicate persistent closed-basin (endorheic) conditions south of the Palomas Basin before Pliocene time. In northern New Mexico, an axial river existed in the Española Basin as early as 13 Ma (Koning and Aby, 2005; Koning, 2007; Koning et al., 2007) and flowed into the Santo Domingo sub-basin by at least 6.9 Ma (Smith et al., 2001; Smith, 2004). This axial river terminated in a playa lake system whose associated lithofacies assemblage is observed in the Popotosa Formation in the southern Albuquerque Basin (Denny, 1940; Bruning, 1973). This playa existed in the Socorro Basin in the latter part of the Miocene (Chamberlin, 1999; Chamberlin and Osburn, 2006).

In the earliest Pliocene, the Rio Grande extended downstream of the Socorro Basin into the Mesilla Basin in southern New Mexico (Mack et al., 1993, 1998, 2006; Connell et al., 2005; Koning et al., 2016a; Repasch et al., 2017). This southward propagation resulted in the fluvial integration of previously endorheic basins that included the Engle, Palomas, Hatch-Rincon, and Mesilla Basins (listed from north to south and shown in Fig. 1). Past work exploring this and other facets of the early Rio Grande include Bryan (1938); Denny (1940), Ruhe (1962), Kottlowski (1953, 1958), Kottlowski et al. (1965), Bachman and Mehnert (1978), Baldrige et al. (1980), Smith et al. (2001), Smith (2004), Connell et al. (2005), and Repasch et al. (2017).

## Previous work

Magnetostratigraphic work by Greg Mack (Mack et al., 1993, 1998, 2006; Leeder et al., 1996) provided key data concerning the age-spatial distribution of axial-fluvial sedimentation in the Palomas and Hatch-Rincon Basins. Figure 2 shows the distribution of oldest ages of exposed axial-fluvial sediments south of TorC. Mack's investigations revealed that the base of exposed axial deposits in the Hatch-Rincon Basin are typically younger than the Gauss-Gilbert Chron boundary (3.6 Ma). This observation has been corroborated by biostratigraphic data from exposures of axial-fluvial strata and interfingering distalmost piedmont deposits, with faunal assemblages ranging from late early Blancan to latest Blancan in age (~3.6–2.0 Ma) (Lucas and Oakes, 1986; Morgan et al., 2011; Morgan and Lucas, 2012; Morgan and Harris, 2015; Morgan et al., unpubl., 2018). Older axial-fluvial sediment is only documented near Garfield, located in the northwestern Hatch-Rincon Basin, and is correlated to the Gilbert Chron (6.0–3.6 Ma). The presence of three normal-polarity subchrons in the Garfield West section, and a reversed polarity interval beneath the lowest subchron (interpreted as the Sidufjall subchron, C3n.3n), strongly suggests that earliest Rio Grande deposition began here between 5.00 and 4.90 Ma (Fig. 2; Mack et al., 1998).

Noteworthy Santa Fe Group exposures north and northwest of downtown TorC were mapped previously by Lozin-

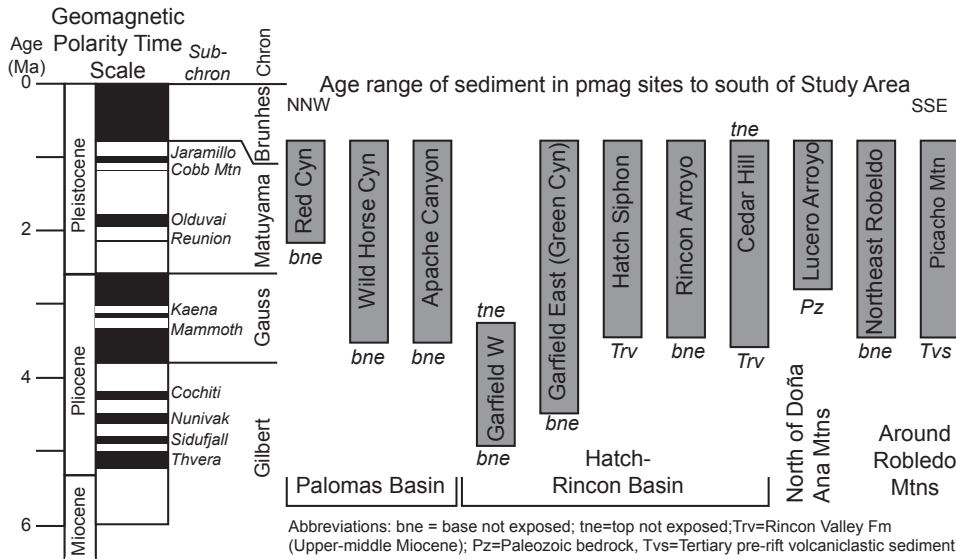


FIGURE 2. Geomagnetic polarity time scale and formal (named) chrons and subchrons for the Plio-Pleistocene (Ogg, 2012). Shaded rectangles indicate interpreted age range of sediment for the paleomagnetic sections shown in Figure 1 (Mack et al., 1993, 1998, 2006). The lower parts of all sections contain axial-fluvial strata. Piedmont strata is found in the upper part of the Red Canyon, Wild Horse Canyon, Apache Canyon, and Garfield East (Green Canyon) stratigraphic sections.

sky (1986), Maxwell and Oakmann (1990), Foster (2009), and Mack et al. (2012). Later detailed sedimentologic and stratigraphic study of exposures immediately north of downtown TorC resulted in differentiation of three distinct axial-fluvial subunits (petrofacies) in the lower ~20 m of early Rio Grande sediment (Fig. 3; Koning et al., 2016a). Age control for these deposits was provided by an <sup>40</sup>Ar/<sup>39</sup>Ar age of 4.87±0.05 Ma on cryptomelane in the Petrofacies unit 2 and a tooth correlated to the Hemphillian horse *Neohipparion eurystyle* in Petrofacies unit 3 (Fig. 3; Koning et al., 2016a). These deposits lie below the Repenning fossil site (~3.6–3.3 Ma per Morgan and Lucas, 2012), but the exact stratigraphic height difference is uncertain due to a 900-m-long projection across a probable fault (Koning et al., 2016a). The relation of these previous data to new stratigraphic observations and geochronologic data is presented below.

**METHODS**

Standard field geology techniques (e.g., Compton, 1985) combined with stereo-photogrammetry was employed to study and map exposures north of Williamsburg (Fig. 4). Lithologic proportions for piedmont lithofacies assemblages were visually estimated and clast counts conducted for gravel compositions. Previously measured stratigraphic sections constrain

lithologic proportions for the axial-fluvial, paleovalley sediment (Koning et al., 2016a). Mansell colors were also visually estimated (and presented in text below) to more effectively differentiate lithologic units. Contacts were plotted using topographic relations on a topographic contour map and using aerial photography obtained from the National Agricultural Imagery Program (NAIP); linework from the latter were interpreted and plotted using photogrammetric ARC software (Stereo Analyst for ArcGIS 10.1, an ERDAS extension, version 11.0.6). Planimetric and vertical accuracy of the NAIP dataset is approximately 5 m (USDA, 2008). Contacts were double-checked by local hand-held GPS measurements. A geologic map was made using ARCGIS v10.3 software, and the

ARC extension stereoanalyst was used to obtain a topographic profile for the new cross-section presented in this paper (Fig. 5).

Two basalt clasts were collected from sedimentary deposits (units Tplt and Tplv, discussed below) in the western study area, immediately west of I-25 (Figs. 4–5). The groundmass concentrate was prepared by treating crushed material with dilute HCl and selecting fragments visibly free of phenocrysts. The basalt samples and monitors (Fish Canyon tuff sanidine, 28.201 Ma, Kuiper et al., 2008) were loaded into aluminum discs and irradiated for 8 hours at the USGS TRIGA reactor in Denver, Colorado. The groundmass was step-heated with a

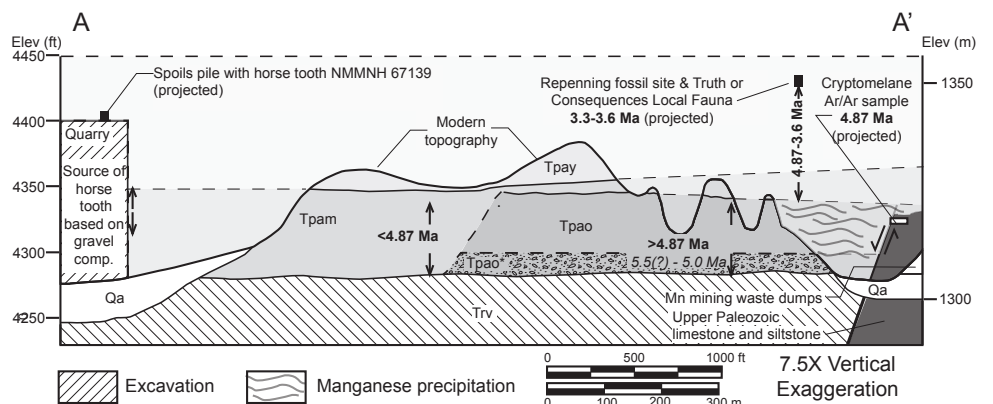


FIGURE 3. Cross-section A-A' showing the butress unconformity between the older and younger paleovalleys backfilled by Tpao and Tpm, respectively. See Figure 4 for cross section line location. Modern topography shown by heavy dark line; lighter lines are horizontally projected contact elevations from exposures within 400 m of the cross-section line (these projections account for the apparent interbedding of Qa with Paleozoic limestone in the lower right of the figure). Local manganese precipitation at one site dated at 4.87±0.05 Ma by <sup>40</sup>Ar/<sup>39</sup>Ar (white rectangle on right side of figure; Koning et al., 2016), is restricted to the older axial-fluvial unit (Tpao). Thus, this unit predates 4.87 Ma. After 4.87 Ma, unit Tpao was incised and then backfilled by the middle axial-fluvial unit (Tpm). At the base of the older axial-fluvial unit lies a coarse conglomerate composed wholly of Paleozoic-Mesozoic sedimentary clasts (Tpa\*). Bold ages are strictly based on biostratigraphic or <sup>40</sup>Ar/<sup>39</sup>Ar constraints; non-bold ages are inferred. Figure is slightly modified from Koning et al. (2016a).

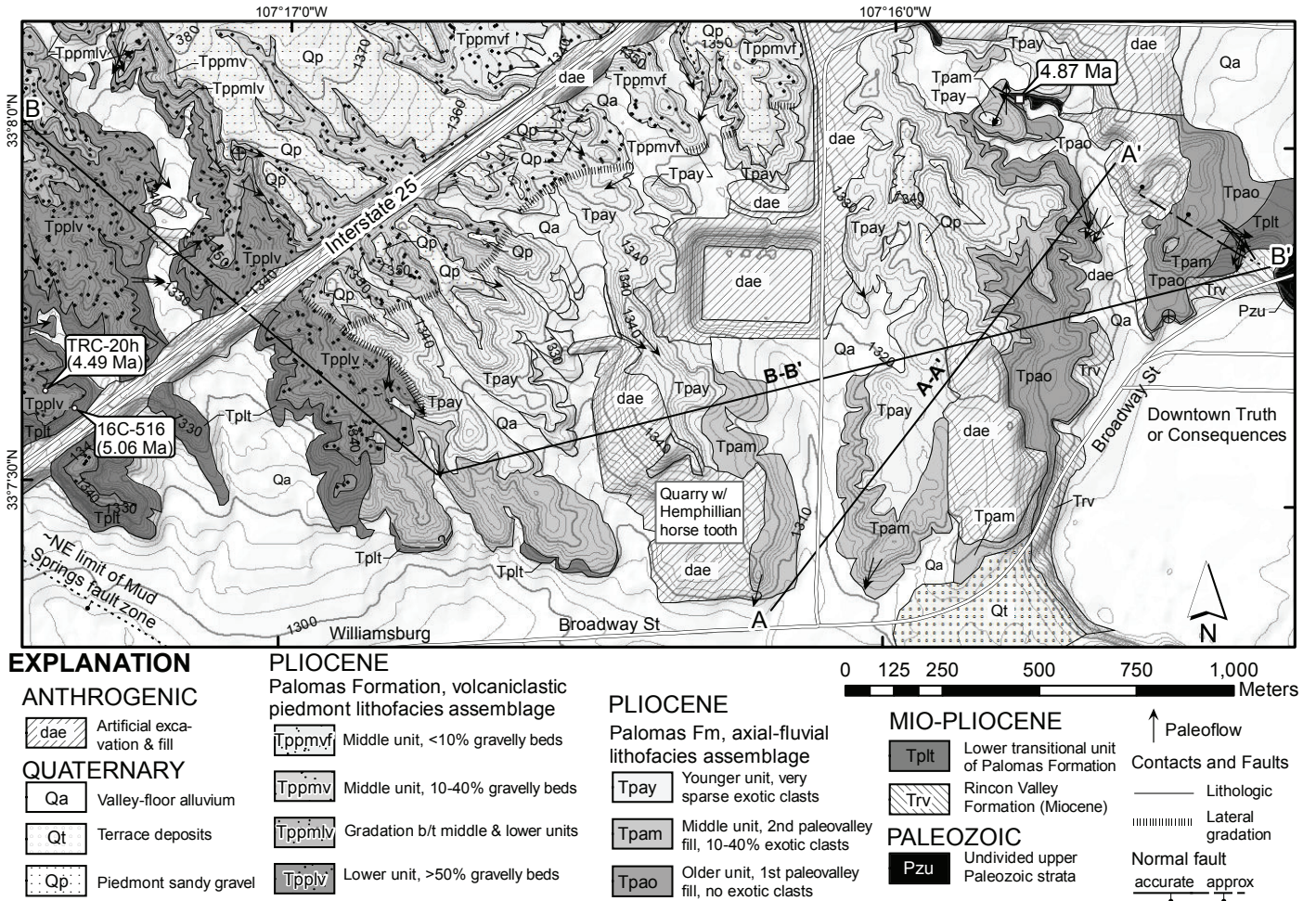


FIGURE 4. Geologic map of the study area. Location of basalt clast samples are shown by labeled open circles. The 4.87±0.05 Ma cryptomelane sample of Koning et al. (2016) is shown by the open square. Map contours and shaded relief constructed using 4.5 m-resolution digital terrain model constructed by Intermap’s STAR technology (Interferometric Synthetic Aperture Radar, or InSAR). Map is part of a larger geologic map of the Cuchillo 7.5-minute quadrangle (Koning et al., 2018).

laser and then analyzed with a mass spectrometer. Instrumental and analytical details are provided in Appendix 1.

**RESULTS**

**Stratigraphy and lithologic descriptions**

Geologic mapping (Fig. 4) and related sedimentologic observations indicate that the studied exposures mostly belong to the piedmont and axial-fluvial lithofacies assemblages of the Palomas Formation, as interpreted by previous workers (Lozinsky, 1986; Foster, 2009; Mack et al., 2012). We have differentiated units within these lithofacies assemblages based largely on texture and gravel composition. Our updated stratigraphy is illustrated in a cross-section drawn across the study area (Fig. 5). Below, we describe the stratigraphic units from oldest to youngest. Stratigraphic labels are keyed to those depicted on the geologic map and cross sections. Detailed descriptions are provided in Koning et al. (2018, note difference in unit nomenclature).

**Rincon Valley Formation**

The Rincon Valley Formation underlies the Palomas Formation axial-fluvial lithofacies assemblage immediately north of

downtown TorC (Koning et al., 2016a). There, the Rincon Valley Formation consists of well-consolidated, medium to thick, tabular beds of claystone-siltstone, clayey-silty sandstone, and minor pebbly sandstone whose colors range from light brown to reddish brown to yellowish red. Paleoflow directions are southerly (ranging 150–215°). Pebbles are angular and composed predominately of locally derived sedimentary clasts, including chert, Paleozoic carbonates (limestone and dolomite), reddish siltstone and very fine-grained sandstone from the Abo Formation, and greenish fine- to medium-grained sandstone from Cretaceous rocks. These gravel compositions are consistent with provenances from the Mud Spring Mountains and the Cuttler Sag area between the Caballo and Fra Cristobal Mountains. The presence of minor granite and gneissic clasts that are very likely derived from the Fra Cristobal Mountains, combined with the southerly paleoflow, was used to interpret that a fluvial system connected the Engle and Palomas Basins prior to arrival of the Rio Grande (Koning et al., 2016a). We have no direct age control for the Rincon Valley Formation, but previous studies interpret it as late Miocene (i.e., Seager et al., 1984; Seager and Mack, 2003).

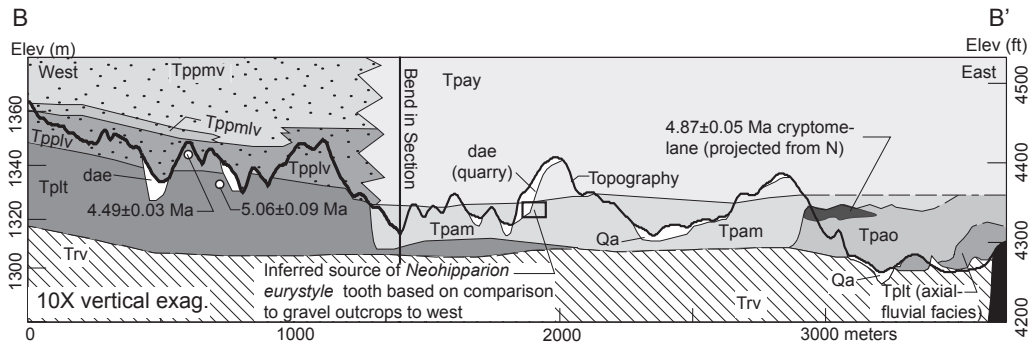


FIGURE 5. Vertically exaggerated (10X) B-B' cross-section across the geologic map of Figure 4, showing stratigraphic relations and the dimensions of the two paleovalleys backfilled by the older and middle axial-fluvial units (Tpao and Tpm, respectively). Shading follows that of Figure 4. Stratigraphic locations of dated basalt clasts are shown by open white circles. Stratigraphic position of the dated cryptomelane precipitation is depicted by the very dark gray shade on the right side of the figure. Note the bend in the section.

### Transitional unit at base of Palomas Formation

Between the Palomas and Rincon Valley Formations lies a ~30-m-thick transitional interval (Tplt on Figs. 4–6) composed of well-consolidated, weakly to strongly cemented sandstone and mudstone that forms bluffs on the north side of Mud Springs Canyon, on either side of I–25. Near the base of these bluffs lies a 0- to 3-m-thick succession composed of thin to thick, tabular beds of light reddish brown to yellowish red (5YR 6/4–5/6), very fine- to medium-grained sandstone, claystone-siltstone, and clayey-silty fine sandstone (commonly horizontal-planar to ripple-laminated). There are minor (~5%) beds composed of very fine- to very coarse-grained sand with 5% pebbles. The fine-grained texture is consistent with a basin floor depositional environment. North of TorC, this unit consists of earliest axial-fluvial strata composed of slightly orangish to white sand interbedded with reddish conglomeratic strata (Koning et al., 2018).

Near I–25, strata overlying the relatively thin basin floor deposits consist of light reddish brown (5YR 6/3–4), medium

to thick, tabular beds composed of: 1) siltstone and very fine- to fine-grained sandstone (about 50–70%); 2) fine- to medium-grained sandstone (~20%); and 3) tabular gravelly complexes whose outcrop proportion increases up-section from 10 to 25% (Fig. 6a), but the gravel proportion decreases laterally northwards. Locally in the finer-grained sandstone there are scattered, coarse sand grains. Gravelly intervals are as much as 2 m thick and consist of thin to medium,

tabular beds composed of pebbly sand or sandy pebbles (with as much as 10% cobbles). Pebbles are composed predominately of volcanic clasts with a visually estimated 1–5% chert and 0–2% granite (both from the Mud Springs Mountains). The proportion of cemented beds increases up-section from 5 to 50%. Cementation is often nodular (5–10 cm across) and probably controlled by bioturbation or burrowing. About 4 m below the upper contact lies a 1–2 m thick, laterally extensive (over several hundred meters), calcium carbonate bed mixed with 20–40% sand and gravel (Fig. 6). Porous features in the calcium carbonate, plus its wide outcrop extent, suggests it is travertine. A basalt clast sample (16C-516, age of  $5.06 \pm 0.02$  Ma) was collected immediately above the travertine alongside I–25 (Figs. 4–5).

### Western piedmont lithofacies assemblage of Palomas Formation

The western piedmont lithofacies assemblage (Tpplv, Tppmlv, Tppmv, and Tppmvf on Fig. 4) is recognized by its volca-

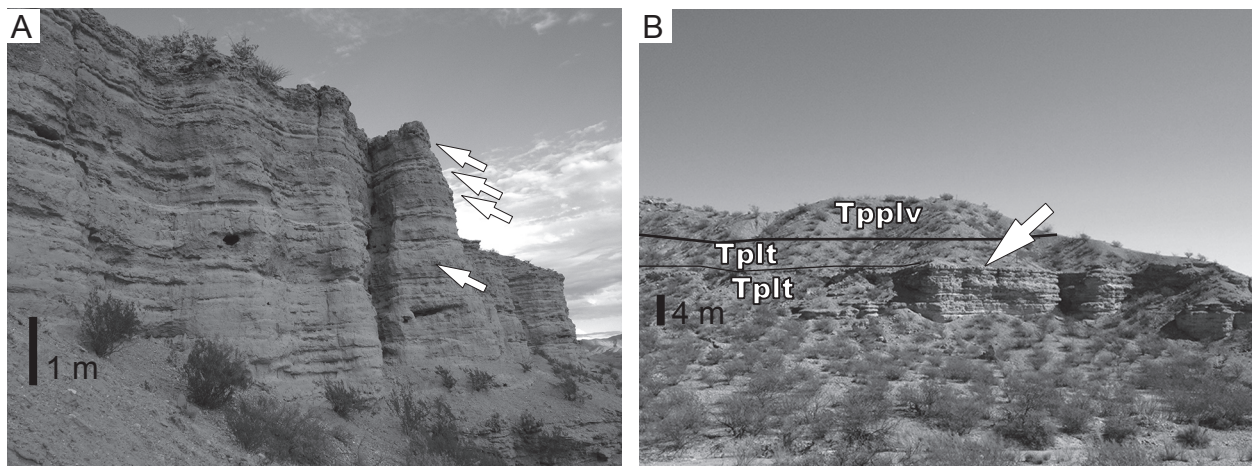


FIGURE 6. Photographs of the 30-m-thick transitional unit at the base of the Palomas Formation (Tplt), located on the west side of the geologic map of Figure 4 near I–25. This unit is coarser than the Rincon Valley Formation, but orangier and less gravelly than the lower, coarse-grained unit of the piedmont volcanoclastic lithofacies assemblage of the Palomas Formation (Tpplv). **A**) View of the transitional unit east-southeast of I–25, showing an up-section increase in the darker conglomeratic beds (latter noted by the white arrows). **B**) Photograph of the lower volcaniclastic unit of the Palomas Formation (Tpplv) overlying the basal Palomas transitional interval (Tplt). White arrow demarcates a laterally extensive (0.5–1.0 km) calcium carbonate bed interpreted to be travertine. Above this travertine lies ~4 m of a conglomerate-bearing interval that coarsens upwards in most places. The 5.1 Ma dated basalt clast (sample 16C-516, Fig. 11) came from the base of this 4-m interval.

nic-dominated conglomerate fraction (subrounded pebbles and subordinate cobbles) that is derived from the Black Range, with very minor gravel contribution from the Mud Springs Mountains. Much of the lower transitional unit of the Palomas Formation can also be assigned to the western piedmont lithofacies assemblage, but we retain it as a separate map unit because of a distinct disconformity coinciding with its upper contact (Fig. 7a). These deposits correspond with the volcanoclastic conglomerate facies assemblage (VCC) of Foster (2009) and Mack et al. (2012). We differentiate four subdivisions of this assemblage based on the proportion of conglomeratic beds. The lower unit (Tpplv) is predominately conglomeratic (Fig. 7a) and the middle unit (Tppmv) contains 20–40% gravelly intervals (over a vertical distance of ~10 m) whose proportion decreases up-section (Fig. 7b). Near I-25, one can map a 3- to 8-m-thick gradational interval between Tpplv and Tppmv, where there are 30–50% gravelly beds (Figs. 4–5). The middle unit (Tppmv) grades laterally northeastward to a finer-grained deposit with <20% gravelly interbeds (Tppmvf); its lowermost strata also interfinger with upper Tplv strata east of I-25. The sand fraction is subrounded to subangular, poorly sorted, commonly exhibits colors of light brown to light reddish brown (5-7.5YR 6/3-4), and its medium- to very coarse-grained fraction is composed predominately of volcanic detritus. The depositional environment for the volcanoclastic lithofacies assemblage corresponds to the distal reaches of an east-sloping piedmont-slope or alluvial fans. The ephemeral drainages were relatively large and sourced in the Black Range (Foster, 2009; Mack et al., 2012).

The western piedmont lithofacies assemblage contains interbedded gravelly beds and gravel-poor beds (<10% gravel). Gravelly intervals are typically tabular and 1–3 m thick (locally up to 6 m). Bedding within these intervals is very thin to medium and lenticular to tabular, with only local cross-stratification. Gravel-poor beds are thin to thick (mostly 10–30 cm thick), tabular, and typically composed of very fine- to medium-grained sandstone and silty-clayey sandstone, with very minor coarse to very coarse sand grains and pebbles scattered

in the finer matrix. Well sorted siltstone and fine-grained sandstone are locally present. Gravel-poor beds are characteristically massive, but have local, very thin to thin lenses of pebbly sand.

#### Axial-fluvial lithofacies assemblage (units Tpao, Tpvf, Tpay)

The three axial-fluvial units (Tpao, Tpvf, Tpay on Fig. 4) described here are generally stratigraphically lower than those described by Foster (2009) and Mack et al. (2012). They are mapped east of I-25 in the study area (Fig. 4). The lower two (Tpao and Tpvf, older and middle axial-fluvial facies, respectively) occupy our two studied paleovalleys and contain more gravelly intervals (15–50%) than the 5–20% estimated gravels in the lower 20 m of the younger unit (Tpay). Unit Tpay conformably overlies unit Tpvf and does not occupy a recognizable paleovalley.

The axial-fluvial lithofacies assemblage is recognized lithologically by its sand fraction, which is relatively well-sorted and quartzo-feldspathic (i.e., mostly quartz, lesser feldspar, and typically <20% lithic, volcanic-dominated grains). In the sand fraction are 1–20% orangish, subrounded grains (which include chert) also observed in outcrop investigations in the Albuquerque and Española Basins. Sand is light-colored (white to light gray to very pale brown), mostly fine- to coarse-grained, subangular to rounded, well-sorted, and lacks notable clay or silt in the matrix.

Three petrofacies have been recognized in the axial-fluvial units, called the Petrofacies units 1–3 in Koning et al. (2016a). The older axial-fluvial unit, occupying the first (oldest) paleovalley, contains both Petrofacies units 1 and 2. Petrofacies unit 1, restricted to the basal 3–8 m of this unit (labeled as Tpao\* in Fig. 3), is coarse conglomerate (abundant cobbles and boulders up to 30 cm in diameter) composed almost entirely of Mesozoic and Paleozoic sedimentary clasts. Petrofacies unit 2 comprises the remainder of the older axial-fluvial unit (Tpao). Its gravel assemblage is mostly composed of felsic volcanic clasts

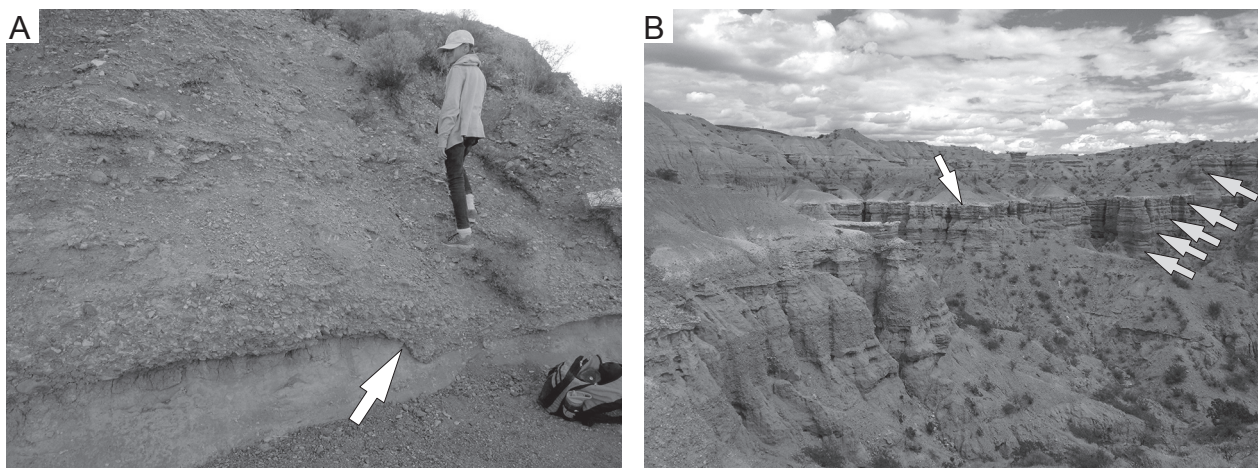


FIGURE 7. Photographs of the lower and middle units of the volcanoclastic lithofacies assemblage of the Palomas Formation. **A**) The lower unit is dominated by volcanoclastic gravels. The white arrow in Photo A points to the scoured unconformity separating the lower unit from the underlying basal Palomas Formation transitional unit. Field assistant is 1.5 m tall. **B**) View of the middle volcanoclastic unit, which has a fining-upward trend. Below the white calcium carbonate bed (shown by the white arrow), gravels (light gray arrows) occupy about a third of the unit but are <30% above the white calcium carbonate bed.

with minor Paleozoic-Mesozoic sedimentary clasts and <3% intermediate volcanic rocks (Koning et al., 2016a, and Koning, unpubl. clast count data). The source areas for these gravel types can be correlated to highlands surrounding the Engle Basin, including the Mud Springs, San Mateo, and Fra Cristobal Mountains (Koning et al., 2016a). The non-gravel fraction consists mainly of fine- to medium-grained sandstone that is horizontal-planar laminated or low-angle cross-laminated. Interbedded in the sandstone is 30–50% conglomerate beds. In the lower-middle part of the unit, the conglomerates are typically massive, with local low-angle cross-stratification, and composed of very fine to very coarse pebbles with minor (10–20%) cobbles in some beds. At the top of the older axial-fluvial unit there are more conglomerate beds and cross-stratification in the gravels is more pronounced (Fig. 8a).

The middle axial-fluvial unit (Tpam), occupying the nested (younger) paleovalley, has a distinctly different gravel assemblage that is coarser than the older and younger units. Gravel occupies an estimated 25–60% of the middle unit and cobbles are more abundant (c.f. Tpao with Tpam in Fig. 8a). The contrast in gravel proportions between Tpam with the overlying, sandier Tpay makes a pronounced topographic bench. The composition of the gravel in the middle axial-fluvial unit corresponds to Petrofacies unit 3 in Koning et al. (2016a). This gravel assemblage has about equal amounts of felsic vs intermediate volcanic rocks, in addition to notable (10–40%) of exotic (extra-basinal) clasts—mainly quartzite and trace Pederal chert (percentages based on clast counts in Koning et al., 2016a). Quartzite is not mapped in the bedrock of local highlands (e.g., mountains around the Engle Basin), and it is likely derived from the Manzano Mountains in central New Mexico or from Proterozoic-cored highlands near Española in northern New Mexico (Koning et al., 2016a; NMBGMR, 2003). Pederal chert is present in the northern Nacimiento Mountains west of Española (Kelley et al., 2013 and references therein). Local cross-stratification sets are thicker than unit Tpay and most of unit Tpao (Fig. 8b). The relatively high proportion of intermediate clasts indicates that much of the volcanic gravel is sourced in the northern Sierra Cuchillo Mountains or the Black Range (Koning et al., 2016a). The increased gravel sizes and presence of exotic clasts in unit Tpam indicate higher paleo-discharges than those associated with Tpao (Koning et al., 2016a).

The lower ~20 m of the younger axial-fluvial unit has a gravel composition similar to the older axial-fluvial unit (i.e., Petrofacies unit 2 of Koning et al., 2016a), with only one exotic-bearing pebble-conglomerate found at the base of the unit near the quarry labeled in Figure 4. Gravels are mainly pebble-size away from the toe of the western piedmont deposits (units Tplv, Tppmv, Tppmvf). Bedding in the lower ~20 m is very thin to medium and tabular-lenticular, with sand beds commonly exhibiting horizontal-planar laminations (Figs. 8c, 8d). Cross-stratification is sparse. Up-section (north of the map area), cross-stratification is more abundant and marked by trough crossbeds 0.2–1.5 m thick (Mack et al., 2012), and clasts of extrabasinal provenance are present.

## Palomas Formation paleovalleys

Stratigraphic relationships presented in the cross-section (Fig. 5) define distinct unconformity bounded packages of sediment that we interpret as buried paleovalleys. These stratigraphic relationships indicate that the middle axial-fluvial unit (Tpam) occupies a paleovalley incised into the transitional unit at the base of the Palomas Formation (steep contact between Tplt and the west side of Tpam, Fig. 5). The eastern part of the older Tpao unit investigated by Koning et al. (2016a) is inset into the transitional lower part of the Palomas Formation north of downtown TorC (near eastern boundary of Fig. 5). North of downtown TorC, the lack of any interfingering between the two unique gravels of the older and middle axial-fluvial units (Tpao and Tpam) and an abrupt lateral transition support earlier interpretations (by Koning et al., 2016a) of a 17- to 19-m-tall buttress unconformity between the two units (Fig. 3). The contact between the middle and older axial-fluvial units corresponds to a buttress unconformity or, up-section, to a more planar (but highly scoured) contact (Figs. 3, 5, 8a). These relations indicate that after 17–20 m of aggradation of the older-fluvial unit (Tpao), there was incision of another paleovalley that was subsequently backfilled by >17 m of the middle axial-fluvial unit (Tpam), whose upper strata onlap Tpao. Our new mapping near I-25 gives unambiguous evidence for a western paleovalley margin (Figs. 5, 9). There, 30 m (exposed thickness) of the orangish, ledge-forming basal Palomas Formation transitional unit (Tplt) is overlain unconformably by the lower-coarse volcanoclastic unit (Tplv). The unconformity can be readily mapped and is characterized by a wavy scour with 1–2 m of relief, across which the units are distinctly different in terms of color, gross texture, and overall cementation (Figs. 6b, 7a). To the east, this contact is steep and forms a buttress unconformity (Figs. 4, 5, 10). To the east of the buttress lies the middle axial-fluvial unit (Tpam), which is >15 m thick (probably ~17 m) and contains 1–10% rounded quartzite clasts (visual estimation) that are characteristic of this unit (Koning et al., 2016a). The diluted quartzite proportion here is likely due to copious input of volcanoclastic sediment from nearby western piedmont drainages. The middle-axial fluvial unit is overlain by the sandier younger axial-fluvial unit (Tpay), which is similar petrologically to the older axial-fluvial unit (Tpao). Above the paleovalley, the younger axial-fluvial unit (Tpay) interfingers westward with the lower and middle volcanoclastic lithofacies assemblage units (Tpplv and Tppmv; Fig. 5).

## Age control

### <sup>40</sup>Ar-<sup>39</sup>Ar results

Gravel samples 16C-516 and TRC-20h yield similar disturbed age spectra (Figs. 10a, b). Both reveal relatively old apparent ages in the early steps that decrease monotonically over the initial 70% of the age spectra: 6.67±0.31 to 5.29±0.01 Ma for sample 16C-516, and 5.55±0.04 to 4.63±0.01 Ma for sample TRC-20h. The final ~30% of the age spectra are relatively flat and yield a calculated weighted mean age of 5.13±0.02 Ma for sample 16C-516 and 4.54±0.02 Ma for sample TRC-

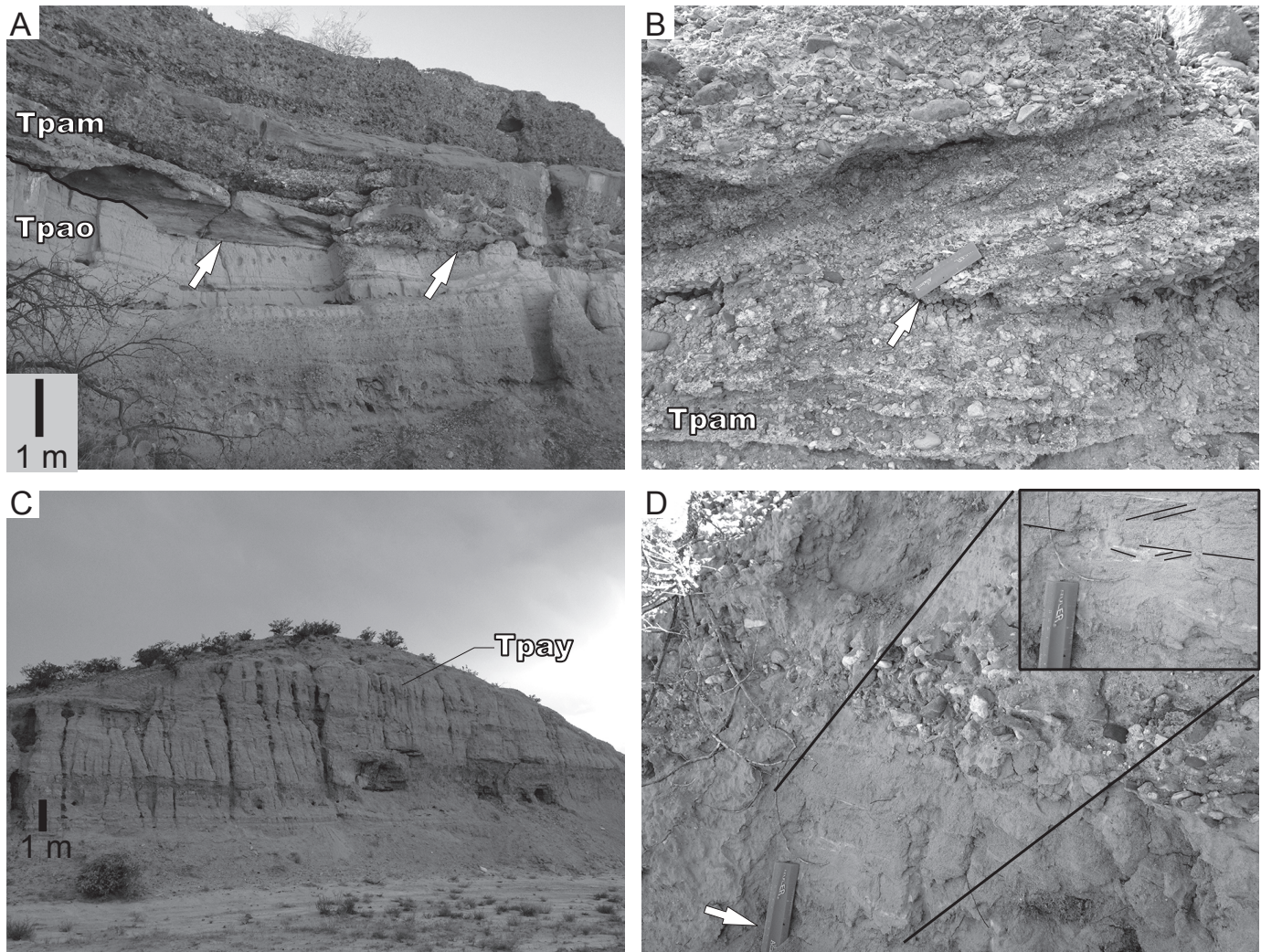


FIGURE 8. Photographs of axial-fluvial units. A) Exposure on the east side of the study area showing a scoured contact (illustrated by the black line and white arrows) separating the older axial-fluvial unit (Tpa0) from the middle axial-fluvial unit (Tpm). These two units have distinctive gravel assemblages, as discussed in text (Koning et al., 2016). Coarse cobbles (128–256 mm max diam) are more common in unit Tpm than in Tpa0. Note the low-angle cross-stratification in unit Tpa0. B) Cross-stratification is more common and thicker in unit Tpm and upper Tpa0 than in younger axial-fluvial deposits. This photograph shows such cross-stratification in unit Tpm near the western buttress of the paleovalley. White arrow points to base of cross-stratification set and a 15-cm-long ruler. C) Sand (mostly very fine- to fine-grained) and clay-silt in tabular beds characterize this 10–13 m tall exposure of the younger axial-fluvial unit, which overlies the paleovalleys. D) A 10- to 30-cm-thick lens of pebbles with ~10–15% fine cobbles interbedded in medium-grained sand, typical of the younger axial-fluvial unit (Tpay). Coarse cobbles are practically absent in Tpay, and cross-stratification is rarely >10 cm thick in the lower part of Tpay. Inset shows annotated horizontal-planar laminations and local ripple marks in the sand. White arrow points to a 15-cm-long ruler.

20h. These flat segments were also investigated by isochron analysis and yield reasonably linear arrays, where TRC-20h provides an isochron age of  $4.49 \pm 0.03$  Ma and 16C-516 is  $5.06 \pm 0.02$  Ma (Figs. 10c, d). The initially old steps of both age spectra are correlated with an increase in radiogenic yield (see top panel showing percent  $^{40}\text{Ar}^*$  in Figs. 11a, b) that supports the likelihood that these increments contain excess argon that may explain the spectra complexity. For instance, steps C-F for sample TRC-20h contain more than 50% of the age spectrum and yield an isochron age of  $4.56 \pm 0.01$  Ma (Fig. 10c) that at 2 sigmas is indistinguishable to the isochron age derived from steps G-M. Steps C-F yield a trapped initial  $^{40}\text{Ar}/^{36}\text{Ar}$  component of  $459 \pm 8$  that is much greater than modern atmosphere at 295.5. Similarly for sample 16C-516, steps C-E project to a trapped excess argon component with an apparent age sub-

equal ( $\pm 2\sigma$ ) to that derived from steps G-M (Fig. 10d). Thus, both dated samples appear to have multiple trapped initial argon components which has been previously documented by Heizler and Harrison (1988). Here, and with the Heizler and Harrison (1988) study, both linear arrays for a given sample yield approximately equal isochron ages but distinct trapped initial components. The preferred eruption age for each sample is given by the isochron arrays calculated for steps G-M, where TRC-20h is  $4.49 \pm 0.03$  Ma and 16C-516 is  $5.06 \pm 0.02$  Ma.

#### Transitional base of Palomas Formation

Dark gray, olivine-phyric, and vesicular basalt clasts, characteristic of Pliocene basalts in the western Palomas Basin (Jochems, 2015; Jochems and Koning, 2016; Koning et al., 2015), provide a means to constrain the age of the transitional

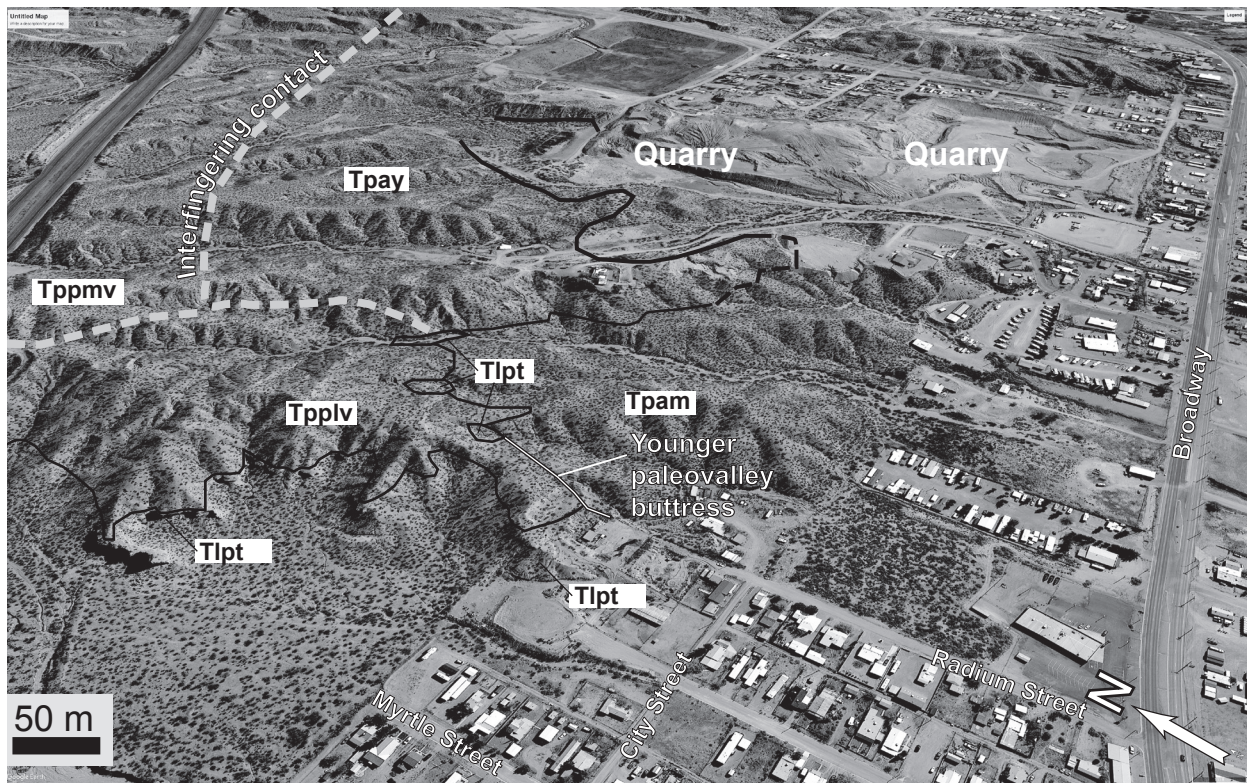


FIGURE 9. Google Earth view of landscape features, geography, and geology near the western butress of the second (younger) paleovalley backfilled by axial-fluvial unit Tpm, which is conformably overlain by the younger axial-fluvial unit (Tpay). Selected Williamsburg street lines are labeled.

unit. The basalt clast (sample 16C-516) collected immediately above the marker calcium carbonate bed (4 m below the top of the unit) has a preferred age of  $5.06 \pm 0.02$  Ma. Thus, the strata overlying the marker calcium carbonate bed must postdate this age.

#### Lower Palomas Formation

$^{40}\text{Ar}/^{39}\text{Ar}$  dating of gravel and a horse tooth fossil help constrain the age of lower Palomas Formation strata west of previous radiometric age control (Koning et al., 2016a). A vesicular, dark gray basalt clast (sample TRC-20h) was collected 6–7 m above the base of the lower coarse volcanoclastic unit (Tpplv). It has a preferred age of  $4.49 \pm 0.03$  Ma, which provides a maximum age for the middle of this 10- to 15-m-thick deposit. Across an interfingering contact, this  $\leq 4.5$  Ma stratigraphic interval projects (parallel to apparent dip) to 10–12 m above the base of the young axial-fluvial unit (Tpay) and  $\sim 11$  m above the top of the western butress of the second paleovalley (Fig. 5). A tooth correlated to *Neohipparion eurystyle* was found in a spoils pile at the north edge of a quarry (Figs. 4–5). The composition and texture (i.e., mostly rounded, very coarse pebbles) of the spoil pile gravel matches *in-situ* gravel observed in the upper part of the middle axial-fluvial unit (Tpm, Figs. 3, 5). Although it is difficult to use the maximum age provided by the basalt clast to tightly constrain the final aggradation of the second paleovalley, the *Neohipparion eurystyle* horse tooth in the paleovalley sediment suggests it probably backfilled by 4.5 Ma (see below).

#### DISCUSSION Paleovalley ages

Early fluvial evolution of the Rio Grande in the TorC area is illustrated by the schematic cross sections of Figure 11. Here, we summarize the age control for this evolution. The presence of the 5.1 Ma basalt clast in the upper 4 m of the basal transitional unit of the Palomas Formation (Tplt) indicates that the upper part of the unit postdates 5.1 Ma. Incision of the paleovalley in which the older axial-fluvial unit (Tpao) was deposited had to occur after 5.1 Ma (the maximum age of the top of Tplt) but before the precipitation of the 4.87 Ma cryptomelane at the top of unit Tpao (Figs. 5, 11). The 17–20 m of aggradation of unit Tpao likewise occurred relatively quickly during 5.1–4.87 Ma.

The 4.87 Ma cryptomelane presented in Koning et al. (2016a) was locally precipitated in the older axial-fluvial unit (Tpao) in a saturated, subsurface environment. The associated manganese precipitation clearly does not extend across a highly scoured contact into overlying unit Tpm (Koning et al., 2016a). The upper part of the paleovalley butress contact was thus eroded after precipitation of the 4.87 Ma cryptomelane. Since incision of the nested paleovalley would have dropped the local water table, we interpret that the 4.87 Ma cryptomelane deposit provides a maximum age for the base of the nested paleovalley (filled by unit Tpm).

A fossilized horse tooth correlated to the middle axial-fluvial unit (Tpm) belongs to a horse species (*Neohipparion eurystyle*; Koning et al., 2016a) interpreted to have first appeared during the late early Hemphillian ( $\sim 7.5$  Ma) and became ex-

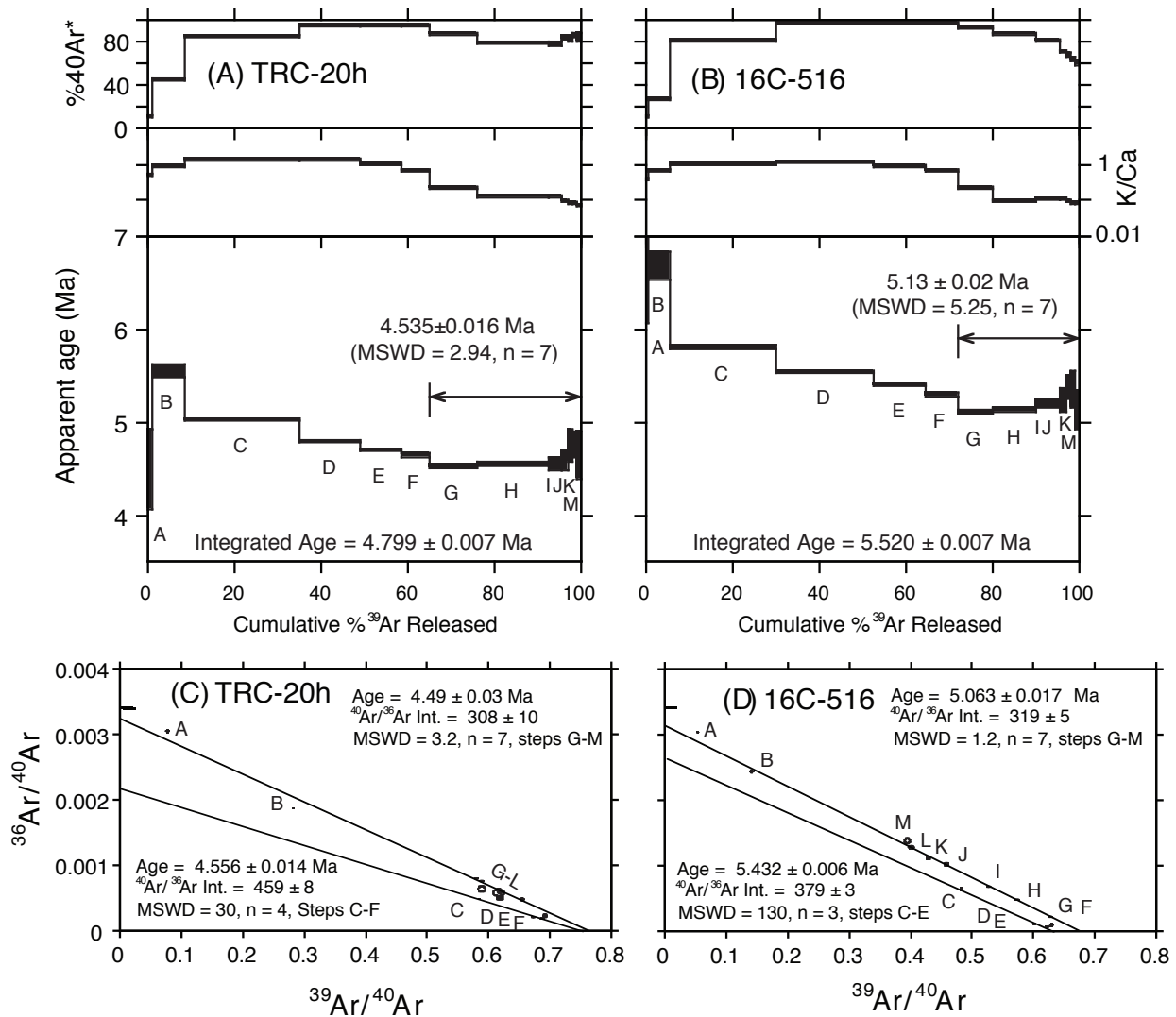


FIGURE 10.  $^{40}\text{Ar}/^{39}\text{Ar}$  diagrams for basalt clast samples TRC-20h and 16C-516. **A, B**) Age spectra, K/Ca and radiogenic yield diagrams ( $\%^{40}\text{Ar}^*$ ). Age spectra reveal decreasing age patterns over much of the spectra with the final ~30% of the  $^{39}\text{Ar}$  released yielding a relatively flat segment. **C, D**) Isochron diagrams revealing multiple trapped initial argon components, with one component (steps C-F in TRC-20h and steps C-E in sample 16C-516) being distinctly excess argon correlating to the old segments of the age spectra and another component nearer to modern atmosphere for the flat segment of each age spectrum. In both samples, steps G-M yield an isochron age that is interpreted to be the eruption age of the sample. The associated analytical data is provided in Appendix 1.

tinct at ~4.9 Ma at the end of the Hemphillian (MacFadden, 1984; Hulbert, 1987). The exact age of this extinction probably has an error of  $\pm 0.1$  Ma, possibly as much as  $\pm 0.2$  Ma (Gary Morgan, NM Museum of Natural History, written commun, 2018), allowing the possibility that the age range of *Neohipparion eurystyle* could extend to 4.8 Ma or, less likely, 4.7 Ma. Using the *Neohipparion eurystyle* tooth to constrain the age of the nested paleovalley is more problematic than using the dated cryptomelane, with two possibilities envisioned: 1) the tooth was not reworked from a notably older deposit, indicating that the younger paleovalley filled quickly between 4.87 and 4.8 Ma (possibly to 4.7 Ma); or 2) the tooth was reworked from a notably older deposit, in which case it only provides a maximum depositional age.

Backfilling of the younger paleovalley occurred after precipitation of the 4.87 Ma cryptomelane, most likely between 4.8 and ca. 4.5 Ma (Fig. 5). The 4.5 Ma age constraint is provided

by the presence of the dated basalt clast in the middle part of the lower coarse volcanoclastic unit (Tpplv) and the eastward projection of this interval to 10–12 m above the base of unit Tpay, the Hemphillian horse tooth in the upper part of Tpm, and the presence of the Repenning fossil site (~3.6–3.3 Ma) >15 m above the base of unit Tpay (see Fig. 4 of Koning et al., 2016a; note that unit Tpay correlates to Tpaou of their work).

#### Causes of paleovalley incision and back-filling

Consistent with interpretations of Koning et al. (2016a), we argue that fluctuating, paleoclimatically modulated discharges of water and sediment were the main drivers for the incision and aggradation of the two paleovalleys observed in the TorC area. Paleoclimate can affect incision and aggradation of a river in several ways that fundamentally relate to the balance between eroding and resisting forces. A river bed that is neither aggrading nor incising is considered to be in an equilibrium



etation (resisting forces to erosion) increased flood magnitudes during intense storms, which could have led to incision of the paleovalleys. Local storm events may have been responsible for incision of the first paleovalley, given the basal cobble-boulder conglomerate derived from local sources. However, the high proportion of extrabasinal gravel (including much cobbles) in the second paleovalley suggests that higher precipitation in the Rio Grande headwaters, coupled with low sediment input from local tributaries, could have promoted incision of the second paleovalley (consistent with the Holocene Rio Grande incision-aggradation conceptual model of Mack et al., 2011). There may also be influences from worldwide early Pliocene paleoclimate changes related to progressive closing of the Indonesian and Panama seaways (Haug and Tiedemann, 1998; Cane and Molnar, 2001; Dowsett et al., 1992; Li et al., 2014) or changes in marine thermohaline circulation (Ravelo and Andreasen, 2000). Circumstantial evidence of probable paleoclimate impacts in western North America during 5.0–4.6 Ma include: 1) the mass extinction event of many mammalian fauna at the boundary between the Hemphillian and Blancan North American land mammal “ages”; and 2) the presence of a particularly coarse deposit (the Bullhead alluvium) in the lower Colorado River during 4.8–4.4 Ma (House et al., 2008; Pearthree and House, 2014), which suggests high stream competencies and paleo-discharges of that river concomitant with the second paleovalley in the lower Rio Grande—which incidentally shares a common headwater in the southern Rocky Mountains.

Alternative drivers for paleovalley formation include base-level drops and unconformities associated with downstream fluvial spillover (e.g., Connell et al., 2017), base-level drops and upstream knickpoint migration from local faulting (Leopold and Bull, 1979; Gardner, 1983; Fenton et al., 2001; Burbank and Anderson, 2012), or epeirogenic uplift (e.g., late Cenozoic incision of the southern Rocky Mountains and western Great Plains; McMillan et al., 2002, 2006; Karlstrom et al., 2012; Leonard, 2002; Eaton, 2008). In regards to unconformities generated by fluvial spillover, there is no evidence that a steep, pre-Rio Grande paleo-topographic gradient existed between the Palomas and Hatch-Rincon Basins (e.g., Plate R5 of Hawley et al., 2005). There is a possibility of a slight(?) paleo-topographic gradient between the Hatch-Rincon and Mesilla Basins, which could have caused an upward propagating knickpoint when the early Rio Grande spilled downstream from the Hatch-Rincon Basin. However, the knickpoint would have had to travel upstream 70 km while maintaining a paleovalley depth of 20 m in soft basin fill.

Base-level drops due to local faulting could induce paleovalley formation on the immediate fault footwall. Immediately southwest of the studied bluffs lies a major rift-flank fault called the Mud Springs fault (Figs. 1, 4). Comparison of 5–1 Ma stratal thickness changes across the fault indicates that the fault was active during this time period at rates of 0.03–0.05 m/my (Koning, unpubl. data), which is slightly lower than the rates associated with incision of the first paleovalley. Moreover, one would expect high rates of base-level drop due to throw along the Mud Springs fault to produce a single paleovalley that would have been backfilled over a prolonged time

period, not two back-to-back, 20-m-scale incision-aggradation events over a 0.6 my time span. Although faulting appears to have been occurring and would have influenced local base level, we assert that rapidly changing ratios of water versus sediment discharge controlled by fluctuating paleoclimate factors provides a more reasonable explanation for the relatively rapid pace of incision and backfilling of these two paleovalleys.

Epeirogenic uplift in northern New Mexico and the southern Rocky Mountains (McMillan et al., 2006; Moucha, 2008; Karlstrom et al., 2012) has been invoked to explain downstream propagation of the Rio Grande in the early Pliocene, either through orogenically enhanced precipitation (Kottlowski, 1953) or increased stream gradients (Repasch et al., 2017). The magnitude of epeirogenic uplift due to mantle-driven processes has been inferred to be 700–750 m since 8–10 Ma (McMillan et al., 2006; Moucha, 2008), which gives an uplift rate of 0.07–0.09 m/ka (0.07–0.09 mm/yr). Considering that the two paleovalleys were formed within 0.6 my, this inferred uplift rate would increase elevation by about 54 m in the headwaters of the Rio Grande, steepening the gradient over the 200 km distance by 0.015°. It is difficult to envision how relatively low rates of epeirogenic uplift would produce significant changes in discharge or sediment flux on timescales of 0.2–0.6 my. Moreover, processes associated with epeirogenic uplift would be expected to consistently supply extrabasinal detritus to the study through steepened channel gradients, which is not observed.

#### **Fortuitous exposure or unique 5.1–4.5 Ma event?**

One might argue that observation of the paleovalleys in in 5.1–4.5 Ma strata near TorC was a result of fortuitous exposures involving unusually distinctive sediment types (within axial-fluvial deposits and between axial-fluvial and piedmont deposits). We counter that post-4.5 Ma axial-fluvial and piedmont deposits are distinctive along the central and southern Rio Grande rift, and past mapping has noted interfingering contacts rather than 20-m-tall buttress relations (e.g., Connell, 2008; Lozinsky, 1986; Jochems and Koning, 2015; Seager and Hawley, 1973; Seager and Mack, 1991; Seager, 1995). Within axial-fluvial deposits, paleovalleys would admittedly be harder to discern. However, mapping of 3 Ma basalt flows intercalated with axial-fluvial facies within the Engle Basin has not revealed thickening of flows consistent with paleovalleys (Cikoski et al., 2017).

#### **Paleovalley between Palomas and Mesilla Basins**

If the two paleovalleys in our study area record 5.1–4.5 Ma hydrologic and geomorphic responses to paleoclimate-modulated fluctuations in sediment versus water discharges, then concomitant paleovalley incision and backfilling may have occurred downstream, particularly in areas of relatively low subsidence rates. Such areas include the Hatch-Rincon Basin and the inter-basinal structural high between the Doña Ana and Robledo Mountains. We suggest that such buried paleovalley(s) may explain the apparent paucity of 4.9–3.6 Ma exposures of axial-fluvial sediment in these aforementioned areas. These deposits could conceivably be buried, but geologic mapping and related cross sections indicate that the base of Camp Rice

Formation axial-fluvial deposits generally is exposed or lies near the base of incised latest Quaternary Rio Grande deposits (Seager and Hawley, 1973; Seager, 1995; Hawley et al., 2005; Jochems, 2017). Another contributing factor is reduced accommodation space due to this area being structurally higher than the Mesilla or Palomas Basins (e.g., Hawley et al., 2005). Earliest Rio Grande spillover from the Palomas Basin may also have contributed to paleovalley formation. According to our conceptual paleovalley model (Fig. 12), incision event(s) between 5.1 and 4.8–4.7 Ma carved a paleovalley(s), and aggradation between 4.8 and 3.6 Ma was largely contained within the paleovalley(s) (cf. Mack et al., 2006, fig. 6). Between 3.6 and 0.8 Ma, axial-fluvial aggradation was more widespread and onlapped the margins of the Hatch-Rincon. After 0.8 Ma, incision of the modern inner valley of the Rio Grande occurred here and across New Mexico (e.g., Connell et al., 2005).

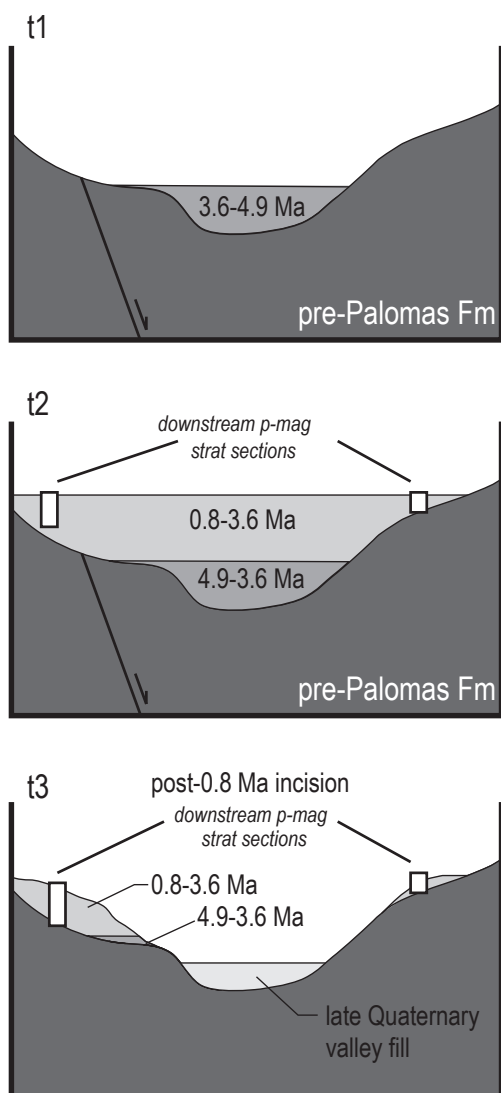


FIGURE 12. Time sequence illustrating our proposed conceptual model of Plio-Pleistocene aggradation in the Hatch-Rincon basin. Postulated paleovalley downstream of the Palomas Basin restricted early (4.9–3.6 Ma) aggradation. During the Gauss chron (3.6–2.6 Ma), axial-fluvial aggradation appreciably onlapped onto the basin margins. During the Brunhes Chron, net incision related to paleoclimatic cycles carved the modern valley.

## CONCLUSION

Geologic mapping near Truth or Consequences (TorC) demonstrates two nested, buried paleovalleys in axial-fluvial deposits of the lower Palomas Formation. Basalt clast ages coupled with previously published geochronology constrain the incision and backfilling of the eastern, older paleovalley to within 5.1 Ma and 4.87 Ma, and the western, younger paleovalley to within 4.87 and ca. 4.5 Ma. Paleoclimate-modulated fluctuations in sediment versus water discharges likely drove these incision-aggradation events, perhaps due to changing atmospheric circulation patterns (e.g., opening of the Gulf of California) that influenced the frequency and magnitude of intense precipitation events or the degree of vegetation cover. Paleovalleys may have confined early (4.9–3.6 Ma) Rio Grande aggradation within relatively narrow belts between the Palomas and Mesilla Basins, and could explain why older axial-fluvial has seldom been recognized in these areas.

## ACKNOWLEDGMENTS

The geologic mapping associated with this work was funded by the STATEMAP program led by J. Michael Timmons at the New Mexico Bureau of Geology & Mineral Resources. We thank Sean Connell and Brian Hampton for reviewing this paper. David Love and Ryan Leary provided a field review on a blustery New Mexico spring day. Claire Koning assisted with measurements of clast imbrications, and Lisa Peters at the NM Geochronology Research Laboratory conducted the  $^{40}\text{Ar}/^{39}\text{Ar}$  age determinations.

## REFERENCES

- Bachman, G.O., and Mehnert, H.H., 1978, New K-Ar dates and the late Pliocene to Holocene geomorphic history of the central Rio Grande region, New Mexico: *Geological Society of America Bulletin*, v. 89, p. 283-292.
- Baldrige, W.S., Damon, P.E., Shafiqullah, M., and Bridwell, R.J., 1980, Evolution of the central Rio Grande rift, New Mexico: New potassium-argon ages: *Earth and Planetary Science Letters*, v. 51, p. 309-321.
- Blum, M.D., and Tornqvist, T.E., 2000, Fluvial responses to climate and sea-level change—a review and look forward: *Sedimentology*, v. 47, p. 2-48.
- Bruning, J.E., 1973, Origin of the Popotosa Formation, north-central Socorro County, New Mexico [Ph.D. dissertation]: Socorro, New Mexico Institute of Mining and Technology, 132 p.
- Bryan, K., 1938, Geology and ground-water conditions of the Rio Grande depression in Colorado and New Mexico: Washington [U.S.] Natural Resources Planning Board, The Rio Grande Joint Investigations in the Upper Rio Grande Basin, v. 1, pt. 2, p. 196-225.
- Bull, W.B., 1991, *Geomorphic Response to Climate Change*: New York, Oxford Press, 326 p.
- Bull, W.B., 1997, Discontinuous ephemeral streams: *Geomorphology*, v. 19, p. 227-276.
- Burbank, D.W., and Anderson, R.S., 2011, *Tectonic Geomorphology*: Hoboken, Wiley-Blackwell, 460 p.
- Cane, M.A., and Molnar, P., 2001, Closing of the Indonesian seaway as a precursor to east African aridification around 3–4 million years ago: *Nature*, v. 411, p. 157-162.
- Chamberlin, R.M., 1999, Geologic map of the Socorro quadrangle, Socorro County, New Mexico: New Mexico Bureau of Geology and Mineral Resources, Open-file Geologic Map 34, scale 1:24,000.
- Chamberlin, R.M., and Osburn, G.R., 2006, Preliminary geologic map of the Water Canyon quadrangle, Socorro County, New Mexico: New Mexico

- Bureau of Geology and Mineral Resources Open-file Geologic Map 118, scale 1:24,000.
- Chapin, C.E., 2008, Interplay of oceanographic and paleoclimate events with tectonism during middle to late Miocene sedimentation across the southwestern USA: *Geosphere*, v. 4, no. 6, p. 976-991.
- Cikoski, C.T., Nelson, W.J., Koning, D.J., Elrick, S., and Lucas, S.G., 2017, Geologic map of the Black Bluffs 7.5-minute quadrangle, Sierra County New Mexico: New Mexico Bureau of Geology and Mineral Resources Open-File Geologic Map 262, scale 1:24,000.
- Compton, R.R., 1985, *Geology in the Field*: New York, John Wiley and Sons, 398 p.
- Connell, S.D., 2008, Geologic map of the Albuquerque-Rio Rancho metropolitan area, Bernalillo and Sandoval County, New Mexico: New Mexico Bureau of Geology and Mineral Resources Geologic Map GM-78, scale 1:50,000, 2 plates.
- Connell, S.D., Hawley, J.W., and Love, D.W., 2005, Late Cenozoic drainage development in the southeastern Basin and Range of New Mexico, southeasternmost Arizona, and western Texas, *in* Lucas, S.G., Morgan, G.S., and Zeigler, K.E., eds., *New Mexico's Ice Ages: New Mexico Museum of Natural History and Science, Bulletin No. 28*, p. 125-150.
- Connell, S., Madof, A.S., and Harris, A.D., 2017, Supply dominated fluvial sequences: implications for sequence stratigraphy in continental settings [abstract]: American Association of Petroleum Geologists Annual Convention and Exhibition, Houston, Texas, AAPG Datapages/Search and Discovery Article: <<http://www.searchanddiscovery.com/abstracts/html/2017/90291ace/abstracts/2601627.html>> (accessed on March 29, 2018).
- Denny, C.S., 1940, Tertiary geology of the San Acacia area, New Mexico: *Journal of Geology*, v. 48, p. 73-106.
- Dethier, D.P., Harrington, C.D., and Aldrich, M.J., 1988, Late Cenozoic rate of erosion in the western Española basin, New Mexico: Evidence from geologic dating of erosion surfaces: *Geological Society of American Bulletin*, v. 100, p. 928-937.
- Dethier, D.P., and Reneau, S.L., 1995, Quaternary History of the western Española Basin, New Mexico: New Mexico Geological Society, Guidebook 46, p. 289-298.
- Dowsett, H.J., Cronin, T.M., Poore, P.Z., Thompson, R.S., Whitley, R.C., et al., 1992, Micropaleontological evidence for increased meridional heat-transport in the North Atlantic Ocean during the Pliocene: *Science*, v. 258, p. 1133-1135.
- Eaton, G.P., 2008, Epeirogeny in the Southern Rocky Mountains region: Evidence and origin: *Geosphere*, v. 4, p. 764-784.
- Ely, L.L., 1997, Response of extreme floods in the southwestern United States to climatic variations in the late Holocene: *Geomorphology*, v. 19, p. 175-201.
- Etheredge, D., Gutzler, D.S., and Pazzaglia, F.J., 2004, Geomorphic response to seasonal variations in rainfall in the southwestern United States: *Geological Society of America Bulletin*, v. 116, p. 606-618.
- Fenton, C.R., Webb, R.H., Pearthree, P.A., Cerling, T.E., and Poreda, R.J., 2001, Displacement rates on the Toroweap and Hurricane faults: Implications for Quaternary downcutting in the Grand Canyon, Arizona: *Geology*, v. 29, p. 1035-1038.
- Foster, R., 2009, Basin-fill architecture of the Pliocene-Lower Pleistocene Palomas Formation adjacent to the intrabasin Mud Springs Mountains, southern Rio Grande rift [unpublished M.S. thesis]: Las Cruces, New Mexico State University, 81 p.
- Gardner, T.W., 1983, Experimental study of knickpoint and longitudinal profile evolution in cohesive, homogeneous material: *Geological Society of America Bulletin*, v. 94, p. 664-672.
- Gile, L.H., Hawley, J.W., and Grossman, R.B., 1981, Soils and geomorphology in the Basin and Range area of southern New Mexico -- Guidebook to the Desert Project: New Mexico Bureau of Mines and Mineral Resources, Memoir 39, 222 p.
- Graf, J.B., Webb, R.H., and Hereford, R., 1991, Relation of sediment load and floodplain formation to climatic variability, Paria River drainage basin, Utah and Arizona: *Geological Society of America Bulletin*, v. 103, p. 1405-1415.
- Graf, W.L., 1988, *Fluvial processes in dryland rivers*: New York, Springer-Verlag, 223 p.
- Haug, G.H., and Tiedemann, R., 1988, Effect of the formation of the Isthmus of Panama on the Atlantic Ocean thermohaline circulation: *Nature*, v. 393, p. 673-676.
- Hawley, J., Kottlowski, F.E., Seager, W.R., King, W.E., Strain, W.S., and Lemone, D.V., 1969, The Santa Fe Group in the south-central New Mexico border region, *in* Kottlowski, F.E., and Lemone, D.V., eds. *Border Stratigraphy Symposium*: New Mexico Bureau of Mines and Mineral Resources Circular 104, p. 52-76.
- Hawley, J.W., Kennedy, J.F., Ortiz, M., and Carrasco, S., 2005, Digital hydrogeologic framework model of the Rincon Valley and adjacent areas of Dona Ana, Sierra, and Luna Counties, *Addendum to N.M.*, Hawley, J.W., and Kennedy, J.F., 2004, Creation of a digital hydrogeologic framework model of the Mesilla Basin and southern Jornada del Muerto Basin: New Mexico Water Resources Research Institute, Technical Completion Report No. 332, 12 p. and 5 Plates in the Addendum.
- Heizler, M.T. and Harrison, T.M., 1988, Multiple trapped argon isotopic components revealed by <sup>40</sup>Ar/<sup>39</sup>Ar isochron analysis: *Geochimica Cosmochimica Acta*, v. 52, p. 295-1303.
- House, P.K., Pearthree, P.A., and Perkins, M.E., 2008, Stratigraphic evidence for the role of lake-spillover in the birth of the lower Colorado River in southern Nevada and western Arizona, *in* Reheis, M.C., et al., eds., *Late Cenozoic draining history of the southwestern Great Basin and lower Colorado River region: Geologic and biotic perspectives*: Geological Society of America, Special Paper 439, p. 335-353.
- Hulbert, R.C., Jr., 1987, Late Neogene Neohipparion (Mammalia, Equidae) from the Gulf Coastal Plain of Florida and Texas: *Journal of Paleontology*, v. 61, p. 809-830.
- Jochems, A.P., 2015, Geologic map of the Williamsburg NW 7.5-minute quadrangle, Sierra County, New Mexico: New Mexico Bureau of Geology, Open-file Geologic Map 251, scale 1:24,000.
- Jochems, A.P., 2017, Geologic map of the Arroyo Cuervo 7.5-minute quadrangle, Sierra County, New Mexico: New Mexico Bureau of Geology, Open-file Geologic Map 261, scale 1:24,000.
- Jochems, A.P., and Koning, D., 2015, Geologic map of the Williamsburg 7.5-minute quadrangle, Sierra County, New Mexico: New Mexico Bureau of Geology, Open-file Geologic Map 250, scale 1:24,000.
- Jochems, A.P., and Koning, D., 2016, Geologic map of the Saladone Tank 7.5-minute quadrangle, Sierra County, New Mexico: New Mexico Bureau of Geology, Open-file Geologic Map 259, scale 1:24,000.
- Jochems, A.P., and Koning, D., 2017, Geologic map of the Clark Spring Canyon 7.5-minute quadrangle, Sierra County, New Mexico: New Mexico Bureau of Geology, Open-file Geologic Map 263, scale 1:24,000.
- Karlstrom, K.E., Coblenz, D., Dueker, K., Ouimet, W., Kirby, E., Van Wijk, J., Schmandt, B., Kelley, S., Lazear, G., Crossey, L.J. and Crow, R., 2012, Surface response to mantle convection beneath the Colorado Rocky Mountains and Colorado Plateau: *Lithosphere*, v. 4, p. 3-22.
- Kelley, S.A., Kemper, K.A., McIntosh, W.C., Maldonado, F., Smith, G.A., Connell, S.D., Koning, D.J., and Whiteis, J., 2013, Syndepositional deformation and provenance of Oligocene to lower Miocene sedimentary rocks along the western margin of the Rio Grande rift, Jemez Mountains, New Mexico, *in* Hudson, M., and Grauch, V.J.S., eds., *New Perspectives on the Rio Grande rift: From Tectonics to Groundwater*: Geological Society of America, Special Paper 494, p. 101-123.
- Knox, J.C., 1983, Responses of river systems to Holocene climates, *in* Wright, H.E., ed., *Late-Quaternary environments of the United States, Volume 2, The Holocene*: Minneapolis, University of Minnesota Press, p. 26-41.
- Knox, J.C., 1993, Large increases in flood magnitude in response to modest changes in climate: *Nature*, v. 361, p. 430-432.
- Knox, J.C., 2000, Sensitivity of modern and Holocene floods to climate change: *Quaternary Science Reviews*, v. 19, p. 439-457.
- Koning, D.J., 2007, Stratigraphic notes on Santa Fe Group exposures west of the Rio Grande between Otowi and Española: New Mexico Geological Society, Guidebook 58, p. 41-43.
- Koning, D.J., and Aby, S.B., 2005, Proposed Members of the Chamita Formation, north-central New Mexico: New Mexico Geological Society, Guidebook 56, p. 258-278.
- Koning, D.J., Aby, S., Grauch, V.J.S., and Zimmerer, M.J., 2016b, Latest Miocene-earliest Pliocene evolution of the ancestral Rio Grande at the Española-San Luis Basin boundary, northern New Mexico: *New Mexico Geology*, v. 38, p. 24-49.
- Koning, D.J., Broxton, D., Sawyer, D., Vaniman, D., and Shomaker, J., 2007, Surface and subsurface stratigraphy of the Santa Fe Group near White Rock and the Buckman areas of the Española Basin, north-central New

- Mexico: New Mexico Geological Society, Guidebook 58, p. 209-224.
- Koning, D.J., Cikowski, C., and Dunbar, N., 2013, Deciphering local landscape stability and surficial processes at a paleovalley margin during a pluvial-interpluvial transition (marine oxygen isotope stages 16-15), central New Mexico: New Mexico Geological Society, Guidebook 64, p. 181-198.
- Koning, D.J., Jochems, A.P., and Cikowski, C., 2015, Geologic Map of the Skute Stone Arroyo 7.5-Minute Quadrangle, Sierra County, New Mexico: New Mexico Bureau of Geology and Mineral Resources, Open-file Geologic Map 252, scale 1:24,000.
- Koning, D.J., Jochems, A.P., Foster, R., Mack, G.H., and Cox, B., 2018, Geologic Map of the Cuchillo 7.5-Minute Quadrangle, Sierra County, New Mexico: New Mexico Bureau of Geology and Mineral Resources, Open-file Geologic Map OF-GM 271, scale 1:24,000.
- Koning, D.J., Jochems, A.P., Morgan, G.S., Lueth, V., and Peters, L., 2016a, Stratigraphy, gravel provenance, and age of early Rio Grande deposits exposed 1-2 km northwest of downtown Truth or Consequences, New Mexico: New Mexico Geological Society, Guidebook 67, p. 459-478.
- Kottlowksi, F.E., 1953, Tertiary-Quaternary sediments of the Rio Grande Valley in southern New Mexico: New Mexico Geological Society, Guidebook 4, p. 144-148.
- Kottlowksi, F.E., 1958, Geologic history of the Rio Grande near El Paso: West Texas Geological Society Guidebook, p. 46-54.
- Kottlowksi, F.W., Cooley, M.E., and Ruhe, R.V., 1965, Quaternary geology of the Southwest, in Wright, H.E., Jr., and Frey, D.G., eds., *The Quaternary Geology of the United States*: Princeton, Princeton University Press, p. 287-298.
- Kuiper, K.F., Deino, A., Hilgen, F.J., Krijgsman, W., Renne, P.R., and Wijbrans, J.R., 2008, Synchronizing rock clocks in Earth history: *Science*, v. 320, p. 500-504.
- Latorre, C., Quade, J., and McIntosh, W.C., 1997, The expansion of C4 grasses and global change in the late Miocene: Stable isotope evidence from the Americas: *Earth and Planetary Science Letters*, v. 146, p. 83-96.
- Lane, E.W., 1955, The importance of fluvial morphology in hydraulic engineering: *Proceedings of the American Society of Civil Engineering*, v. 81, p. 1-17.
- Langbein, W.B., and Schumm, S.A., 1958, Yield of sediment in relation to mean annual precipitation: *American Geophysical Union Transactions*, v. 39, p. 1076-1084.
- Leeder, M.R., Mack, G.H., and Salyards, S.L., 1996, Axial-transverse fluvial interactions in a half-graben: Plio-Pleistocene Palomas basin, southern Rio Grande rift, New Mexico, USA: *Basin Research*, v. 12, p. 225-221.
- Leonard, E.M., 2002, Geomorphic and tectonic forcing of late Cenozoic warping of the Colorado Piedmont: *Geology*, v. 30, p. 595-598.
- Leopold, L.B., 1951a, Vegetation of southwestern watersheds in the nineteenth century: *Geographical Review*, v. 41, p. 295-316.
- Leopold, L.B., 1951b, Rainfall frequency: An aspect of climatic variation: *American Geophysical Union Transactions*, v. 32, p. 347-357.
- Leopold, L.B., and Bull, W.B., 1979, Base level, aggradation, and grade: *American Philosophical Society Proceedings*, v. 123, p. 168-202.
- Li, F., Wu, N., Rousseau, D-D, Dong, Y., Zhang, D., and Pei, Y., 2014, Late Miocene-Pliocene paleoclimatic evolution documented by terrestrial mollusk populations in the western Chinese Loess Plateau: *PLoS One*, v. 9 (4), e95754.
- Lozinsky, R.P., 1986, Geology and late Cenozoic history of the Elephant Butte area, Sierra County, New Mexico: New Mexico Bureau of Mines and Mineral Resources Circular 187, 39 p.
- Lozinsky, R.P., and Hawley, J.W., 1986a, The Palomas Formation of south-central New Mexico—A formal definition: *New Mexico Geology*, v. 8, p. 73-82.
- Lozinsky, R.P., and Hawley, J.W., 1986b, Upper Cenozoic Palomas Formation of south-central New Mexico: New Mexico Geological Society, Guidebook 37, p. 239-247.
- Lucas, S.G., and Oakes, W., 1986, Pliocene (Blancan) vertebrates from the Palomas Formation, south-central New Mexico: New Mexico Geological Society, Guidebook 37, p. 249-263.
- MacFadden, B.J., 1984, Systematics and phylogeny of *Hipparion*, *Neohipparion*, *Nannippus*, and *Cormohipparion* (Mammalia, Equidae) from the Miocene and Pliocene of the New World: *Bulletin of the American Museum of Natural History*, v. 171, p. 1-195.
- MacFadden, B.J., 1992, Fossil horses: Systematics, paleobiology, and evolution of the family Equidae: New York, Cambridge University Press, 369 p.
- Mack, G.H., 2004, Middle and late Cenozoic crustal extension, sedimentation, and volcanism in the southern Rio Grande rift, Basin and Range, and southern transition zone of southwestern New Mexico, in Mack, G.H., and Giles, K.A., eds., *The Geology of New Mexico, A Geologic History*: New Mexico Geological Society, Special Publication 11, p. 389-406.
- Mack, G.H., Foster, R., and Tabor, N.J., 2012, Basin architecture of Pliocene-lower Pleistocene alluvial-fan and axial-fluvial strata adjacent to the Mud Springs and Caballo Mountains, Palomas half graben, southern Rio Grande rift: New Mexico Geological Society, Guidebook 63, p. 431-445.
- Mack, G.H., Leeder, M., Perez-Arllucea, M., and Durr, M., 2011, Tectonic and climatic controls on Holocene channel migration, incision and terrace formation by the Rio Grande in the Palomas half graben, southern Rio Grande rift, USA: *Sedimentology*, v. 58, p. 1065-1086.
- Mack, G.H., Salyards, S.L., and James, W.C., 1993, Magnetostratigraphy of the Plio-Pleistocene Camp Rice and Palomas Formations in the Rio Grande rift of southern New Mexico: *American Journal of Science*, v. 293, p. 49-77.
- Mack, G.H., Salyards, S.L., McIntosh, W.C., and Leeder, M.R., 1998, Reversal magnetostratigraphy and radioisotopic geochronology of the Plio-Pleistocene Camp Rice and Palomas formations, southern Rio Grande rift: New Mexico Geological Society, Guidebook 49, p. 229-236.
- Mack, G.H., Seager, W.R., and Kieling, J., 1994, Late Oligocene and Miocene faulting and sedimentation, and evolution of the southern Rio Grande rift, New Mexico, USA: *Sedimentary Geology*, v. 92, p. 79-96.
- Mack, G.H., Seager, W.R., Leeder, M.R., Perez-Arllucea, M., and Salyards, S.L., 2006, Pliocene and Quaternary history of the Rio Grande, the axial river of the southern Rio Grande rift, New Mexico, USA: *Earth-Science Reviews*, v. 79, p. 141-162.
- Mann, D.H., and Meltzer, D.J., 2007, Millennial-scale dynamics of valley fills over the past 12,000 <sup>14</sup>C yr in northeastern New Mexico: *Geological Society of America Bulletin*, v. 119, p. 1433-1448.
- Maxwell, C.H., and Oakman, M.R., 1990, Geologic map of the Cuchillo quadrangle, Sierra County, New Mexico: United State Geological Survey Geologic Quadrangle Map GQ-1686, scale 1:24,000.
- McMillan, M.E., Angevine, C.L., and Heller, P.L., 2002, Postdepositional tilt of the Miocene-Pliocene Ogallala Group on the western Great Plains: Evidence of late Cenozoic uplift of the Rocky Mountains: *Geology*, v. 30 p. 63-66.
- McMillan, M.E., Heller, P.L., and Wing, S.L., 2006, History and causes of post-Laramide relief in the Rocky Mountain orogenic plateau: *Geological Society of America Bulletin*, v. 118, p. 393-405.
- Meyer, G.A., Wells, S.G., and Jull, A.J.T., 1995, Fire and alluvial chronology in Yellowstone National Park: Climate and intrinsic controls on Holocene geomorphic processes: *Geological Society of America Bulletin*, v. 107, p. 1211-1230.
- Morgan, G.S., and Harris, A.H., 2015, Pliocene and Pleistocene vertebrates of New Mexico, in Lucas, S.G., and Sullivan, R.B., eds., *Vertebrate Paleontology in New Mexico*: New Mexico Museum of Natural History and Science Bulletin 68, p. 233-427.
- Morgan, G.S., and Lucas, S.G., 2012, Cenozoic vertebrates from Sierra County, southwestern New Mexico: New Mexico Geological Society, Guidebook 63, p. 525-540.
- Morgan, G.S., Sealey, P., and Lucas, S.G., 2011, Pliocene and early Pleistocene (Blancan) vertebrates from the Palomas Formation in the vicinity of Elephant Butte Lake and Caballo Lake, Sierra County, southwestern New Mexico: New Mexico Museum of Natural History and Science Bulletin 53, p. 664-736.
- Moucha, R., Forte, A.M., Rowley, D.B., Mitrovica, J.X., Simmons, N.A., and Grand, S.P., 2008, Mantle convection and the recent evolution of the Colorado Plateau and the Rio Grande Rift valley: *Geology*, v. 36, p. 439-442.
- NMBGMR [New Mexico Bureau of Geology and Mineral Resources], 2003, *Geologic Map of New Mexico*: New Mexico Bureau of Geology and Mineral Resources, scale 1:500,000.
- Ogg, J.G., 2012, Geomagnetic polarity time scale, in Gradstein, F.M., Ogg, J.G., Schmitz, M.D., and Ogg, G.M., eds., *The Geologic Time Scale 2012*: New York, Elsevier, p. 31-42.
- Pazzaglia, F.J., 2005, River responses to Ice Age (Quaternary) climates in New Mexico, in Lucas, S.G., Morgan, G.S., and Zeigler, K.E., eds., *New Mexico's Ice Ages*: New Mexico Museum of Natural History and Science, Bulletin No. 28, p. 115-124.

- Pearthree, P.A., and House, P.K., 2014, Paleogeomorphology and evolution of the early Colorado River inferred from relationships in Mohave and Cottonwood valleys, Arizona, California, and Nevada: *Geosphere*, v. 10, no. 6, p. 1139-1160; doi: 10.1130/GES00988.1.
- Ravelo, A.C., and Andreason, D.H., 2000, Enhanced circulation during a warm period: *Geophysical Research Letters*, vol. 27, no. 7, p. 1001-1004.
- Repasch, M., Karlstrom, K., Heizler, M., and Pecha, M., 2017, Birth and evolution of the Rio Grande fluvial system in the past 8 Ma: Progressive downward integration and the influence of tectonics, volcanism, and climate: *Earth-Science Reviews*, v. 168, p. 113-164, doi: 10.1016/j.earscirev.2017.03.003.
- Rogers, J.B., and Smartt, R.A., 1996, Climatic influences on Quaternary alluvial stratigraphy and terrace formation in the Jemez River valley, New Mexico: N.M. Geological Society, 47th Field Conference Guidebook, p. 347-356.
- Ruhe, 1962, Age of the Rio Grande Valley in southern New Mexico: *Journal of Geology*, v. 70, issue 2, p. 151-167.
- Schumm, S.A., 1977, *The Fluvial System*: New York, John Wiley and Sons, 338 pp.
- Schumm, S.A., and Hadley, R.F., 1957, Arroyos and the semiarid cycle of erosion: *American Journal of Science*, v. 255, p. 161-174.
- Schumm, S.A., and Parker, R.S., 1973, Implications of complex response of drainage systems for Quaternary alluvial stratigraphy: *Nature Physical Science*, v. 243, p. 99-100.
- Seager, W.R., 1995, Geologic map of the Hatch quadrangle, Dona County, New Mexico: New Mexico Bureau of Geology and Mineral Resources, Open-file Geologic Map OF-GM 213, scale 1:24,000.
- Seager, W.R., 2015, Geologic map of the Palomas Gap 7.5-minute quadrangle, Sierra County, New Mexico: New Mexico Bureau of Geology and Mineral Resources, Open-file Geologic Map OF-GM 260, scale 1:24,000.
- Seager, W.R., Clemons, R.E., and Hawley, J.W., 1975, Geology of Sierra Alta quadrangle, Doña Ana County, New Mexico: New Mexico Bureau of Mines and Mineral Resources, Bulletin 102, 56 p. and 1 plate.
- Seager, W.R., Clemons, R.E., Hawley, J.W., and Kelley, R.E., 1982, Geology of the northwest part of the Las Cruces 1° x 2° sheet, New Mexico: New Mexico Bureau of Mines and Mineral Resources, Geologic Map 53, scale 1:125,000.
- Seager, W. R. and Hawley, J. W., 1973, Geology of Rincon quadrangle, New Mexico: New Mexico Bureau of Mines and Mineral Resources, Bulletin 101, 42 p., map scale 1:24,000.
- Seager, W.R., Hawley, J.W., and Clemons, R.E., 1971, Geology of San Diego Mountain area, Doña Ana County, New Mexico: New Mexico Bureau of Mines and Mineral Resources, Bulletin 97, 38 p. and 2 plates.
- Seager, W.R., and Mack, G.H., 1991, Geology of the Garfield quadrangle, Sierra and Dona Ana Counties, New Mexico: Mexico Bureau of Mines and Mineral Resources Bulletin 128, 24 p., map scale 1:24,000.
- Seager, W.R., and Mack, G.H., 2003, Geology of the Caballo Mountains, New Mexico: New Mexico Bureau of Geology and Mineral Resources Memoir 49, 136 p.
- Seager, W.R., Shafiqullah, M., Hawley, J.W., and Marvin, R.F., 1984, New K-Ar dates from basalts and the evolution of the southern Rio Grande rift: *Geological Society of America Bulletin*, v. 95, no. 1, p. 87-99.
- Sklar, L.S., and Dietrich, W.E., 2001, Sediment and rock strength controls on river incision into bedrock: *Geology*, v. 29, p. 1087-1090.
- Smith, G.A., 2004, Middle to late Cenozoic development of the Rio Grande rift and adjacent regions in northern New Mexico, *in* Mack, G.H., and Giles, K.A., eds., *The Geology of New Mexico, A Geologic History*: New Mexico Geological Society Special Publication 11, p. 331-358.
- Smith, G.A., McIntosh, W., and Kuhle, A.J., 2001, Sedimentologic and geomorphic evidence for seesaw subsidence of the Santo Domingo accommodation-zone basin, Rio Grande rift, New Mexico: *Geological Society of America Bulletin*, v. 113, no. 5, p. 561-574.
- Thompson, R.S., 1991, Pliocene environments and climates in the western United States: *Quaternary Science Reviews*, v. 10, issue 2-3, p. 115-132.
- Tucker, G.E., Arnold, L., Bras, R.L., Flores, H., Istanbuluoglu, E., and Solyom, P., 2006, Headwater channel dynamics in semiarid rangelands, Colorado high plains, USA: *Geological Society of America Bulletin*, v. 118, p. 959-974.
- USDA, 2008, Natural Agricultural Imagery Program (NAIP) factsheet: U.S. Department of Agriculture, U.S. Department of Agriculture, 2 p.
- Webb, S.D., and Opdike, N.D., 1995, Global climatic influence on Cenozoic land mammal faunas, *in* *Effects of past global change on life*: Washington, D.C., National Academy Press, p. 184-208.

Supplemental data can be found at <http://nmgs.nmt.edu/repository/index.cfm?rid=2018001>